S K-edge X-ray Absorption Studies of Tetranuclear Iron−Sulfur Clusters: μ-Sulfide Bonding and Its Contribution to Electron Delocalization

Thorsten Glaser,[†] Kendra Rose,[†] Susan E. Shadle,[†] Britt Hedman,*[,†,‡] Keith O. Hodgson,*[,†,‡] and Edward I. Solomon*[,†]

Contribution from the Department of Chemistry, Stanford University, Stanford, California 94305, and Stanford Synchrotron Radiation Laboratory, SLAC, Stanford University, Stanford, California 94309

Received June 19, 2000. Revised Manuscript Received October 16, 2000

Abstract: X-ray absorption spectroscopy (XAS) at the sulfur (~2470 eV) and chlorine (~2822 eV) K-edges has been applied to a series of 4Fe−4S model complexes. These are compared to 2Fe−2S model complexes to obtain insight into the *localized* ground state in the mixed-valence dimer versus the *delocalized* ground state in the mixed-valence tetramer. The preedges of hypothetical delocalized mixed-valence dimers $[Fe_2S_2]^+$ are estimated using trends from experimental data and density functional calculations, for comparison to the delocalized mixed-valence tetramer $[Fe_4S_4]^{2+}$. The differences between these two mixed-valence sites are due to the change of the sulfide-bridging mode from μ_2 to μ_3. The terminal chloride and thiolate ligands are used as spectator ligands for the electron density of the iron center. From the intensity of the preedge, the covalency of the terminal ligands is found to increase in the tetramer as compared to the dimer. This is associated with a higher effective nuclear charge on the iron in the tetramer (derived from the energies of the preedge). The μ_3-bridging sulfide in the tetramer has a reduced covalency per bond (39%) as compared to the μ_2-bridging sulfide in the dimer (51%). A simple perturbation model is used to derive a quadratic dependence of the superexchange coupling constant J on the covalency of the metal ions with the bridging ligands. This relationship is used to estimate the superexchange contribution in the tetramer ($J = -156$ cm^{-1}) as compared to the mixed-valence dimer ($J = -360$ cm^{-1}). These results, combined with estimates for the double exchange and the vibronic coupling contributions of the dimer sub-site of the tetramer, lead to a delocalized $S_t = {}^9/_2$ spin ground state for the mixed-valence dimer in the tetramer. Thus, the decrease in the covalency, hence the superexchange pathway associated with changing the bridging mode of the sulfides from μ_2 to μ_3 on going from the dimer to the tetramer, significantly contributes to the delocalization of the excess electron over the dimer sub-site in the tetramer.

Introduction

Biological systems extensively employ iron−sulfur (Fe−S) clusters for electron transfer, catalysis, and other functions such as oxygen-sensing and DNA regulation. Their biochemistry and electronic structures have been studied in great detail, and excellent reviews are available.[1−6] The four most common structural types of iron−sulfur clusters with 1−4 iron centers are shown in Scheme 1. The simplest of the Fe−S proteins are the rubredoxins, which contain one iron center coordinated by four cysteines. In the 2Fe ferredoxins, the metal ions have two terminal cysteine ligands and two μ_2-bridging sulfides. Each iron center in the 4Fe ferredoxins and HiPIPs (high potential iron proteins) has one terminal thiolate and is bridged by three sulfides in μ_3-bridging modes.

Scheme 1

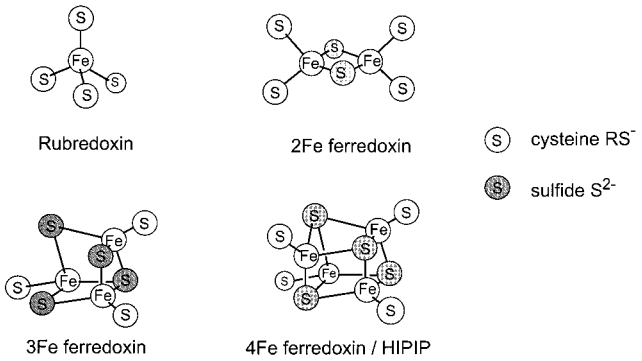

All iron ions are in a high spin ferrous or ferric electron configuration. In the 2Fe ferredoxins, the iron centers are antiferromagnetically coupled through a superexchange pathway via the bridging sulfides. The biologically relevant redox reaction of the 2Fe ferredoxins involves a one-electron couple between Fe^{III}/Fe^{III} and Fe^{III}/Fe^{II}. The oxidized site has an $S_t = 0$ ground state, while the reduced state, which is a localized mixed-valence site (class II in the nomenclature of Robin and

* To whom correspondence should be addressed.
[†] Department of Chemistry, Stanford University.
[‡] Stanford Synchrotron Radiation Laboratory, Stanford University.

(1) Beinert, H. *J. Biol. Inorg. Chem.* **2000**, *5*, 2−15.
(2) Beinert, H.; Holm, R. H.; Münck, E. *Science* **1997**, *277*, 653−659.
(3) *Iron-Sulfur Proteins*; Lovenberg, W., Ed.; Academic Press: New York, 1973−1977; Vols. I−III.
(4) *Iron-Sulfur Proteins*; Spiro, T. G., Ed.; Metal Ions In Biology, Vol. IV; Wiley-Interscience: New York, 1982.
(5) *Iron-Sulfur Proteins*; Cammack, R., Ed.; Advances in Inorganic Chemistry, Vol. 38; Academic Press: San Diego, 1992.
(6) *Iron-Sulfur Proteins*; Sykes, A. G., Cammack, R., Eds.; Advances in Inorganic Chemistry, Vol. 47; Academic Press: San Diego, 1999.

10.1021/ja002183v CCC: $20.00
Published on Web 12/28/2000

Day[7]), has an $S_t = {}^1/_2$ ground state. The clusters with four iron sites occur naturally in three different oxidation states, $[Fe_4S_4]^{1+}$, $[Fe_4S_4]^{2+}$, and $[Fe_4S_4]^{3+}$. The 4Fe ferredoxins function between the first two redox states whereas the HiPIPs utilizes the 2+/3+ couple. The $[Fe_4S_4]^{2+}$ oxidation state formally consists of 2 Fe^{III} and 2 Fe^{II} ions. However, it was found experimentally that all four iron centers are in the same formal oxidation state, which is generally considered to be $Fe^{2.5}$.[2] The tetrameric Fe−S clusters are viewed as a dimer of two mixed-valence delocalized sub-dimers (class III mixed valence). The excess electron is delocalized over both iron centers of the $Fe^{III}Fe^{III}$ core. Thus, in going from the mixed-valence dimer to the mixed-valence tetramer, the localized excess electron in the dimer delocalizes over the dimer sub-sites in the tetramer.

The delocalization of the excess electron in the mixed-valence state is accompanied by a net ferromagnetic coupling between the iron centers leading to a $S_t = {}^9/_2$ dimer ground state. This phenomenon of spin alignment in mixed-valence systems with delocalized ground states is called double exchange in analogy to Kramer's superexchange mechanism.[8,9] The physical origin of double exchange elucidated by Girerd, Münck and co-workers,[10−12] and Noodleman and Baerends,[13] is that electron transfer leads to a loss of spin polarization energy for the antiferromagnetic but not for the ferromagnetic configuration.[13] There are three types of interactions to consider between the magnetic centers in a mixed-valence pair, namely superexchange (parametrized by J (using $H = -2J\mathbf{S}_1\mathbf{S}_2$)), double exchange ($B$), and vibronic coupling (Λ^2/k_-). The energies of the spin states are given by:

$$E_{\pm}(S_T) = -JS_T(S_T+1) + \frac{1}{2}\left(\frac{\Lambda^2}{k_-}\right)x_-{}^2 \pm \sqrt{\frac{1}{2}\left(\frac{\Lambda^2}{k_-}\right)^2 x_-{}^2 + B^2\left(S_T+\frac{1}{2}\right)^2} \quad (1)$$

Superexchange leads mainly to antiferromagnetic coupling, whereas double exchange leads to delocalization of the excess electron and to ferromagnetic coupling. Vibronic coupling is the driving force for localization of the excess electron. The interplay between these three interactions leads to interesting potential energy surfaces for the spin states in the antisymmetric breathing mode Q_-.[14] Double exchange, as the driving force for electron delocalization, is more effective in the higher spin states. Thus, strong superexchange, which leads to a stabilization of the lower spin states, makes the double exchange less effective and thus indirectly decreases the tendency for electron delocalization.

It has been considered that the delocalization of the excess electron in the mixed-valence sub-dimers of $[3Fe-4S]^0$ and $[4Fe-4S]^{1+,2+,3+}$ originates from spin frustration. The spins in these clusters cannot all be aligned antiferromagnetically due to the presence of three or four equal spin centers. This spin frustration leads to parallel alignment of two of the spins. The parallel spin alignment makes the double exchange interaction more effective, leading to the delocalized sub-dimers.[15]

The mixed-valence model compound $[LFe(\mu\text{-}OH)_3FeL]^{2+}$ (L = 1,4,7-trimethyl-1,4,7-triazacyclononane) synthesized by Wieghardt, Chaudhuri, and co-workers[19] consists formally of one Fe^{III} and one Fe^{II} ion, but was shown to be a class III fully delocalized $Fe^{2.5}Fe^{2.5}$ mixed-valence dimer with a ferromagnetic $S_t = {}^9/_2$ spin ground state.[20,21] Thus, delocalization of the excess electron with parallel spin alignment is possible in a dimer without spin frustration. Analogously, it was shown that an excess electron delocalizes over three metal centers in linear mixed-valence trimers without the occurrence of spin frustration.[22,23] A spectroscopic study comparing the delocalized mixed-valence model $[LFe(\mu\text{-}OH)_3FeL]^{2+}$ with the localized mixed-valence dimer $[2Fe-2S]^+$ showed that the main difference between these two is the reduced superexchange coupling in the $[LFe(\mu\text{-}OH)_3FeL]^{2+}$ model as compared to the Fe−S dimer, due to the reduced covalency of the protonated bridging ligands with the metal centers.[24,25]

A direct experimental probe of ligand−metal bonding interactions is provided by ligand K-edge X-ray absorption spectroscopy (XAS).[26−38] The electric dipole-allowed transitions for

(7) Robin, M. B.; Day, P. *Adv. Inorg. Chem. Radiochem.* **1967**, *10*, 247−422.
(8) Zener, C. *Phys. Rev.* **1951**, *82*, 403−405.
(9) Kramer, A. *Physica* **1934**, *1*, 191−192.
(10) Girerd, J.-J. *J. Chem. Phys.* **1983**, *79*, 1766−1775.
(11) Papaefthymiou, V.; Girerd, J. J.; Moura, I.; Moura, J. J. G.; Münck, E. *J. Am. Chem. Soc.* **1987**, *109*, 4703−4710.
(12) Blondin, G.; Girerd, J. J. *Chem. Rev.* **1990**, *90*, 1359−1376.
(13) Noodleman, L.; Baerends, E. J. *J. Am. Chem. Soc.* **1984**, *106*, 2316−2327.
(14) The parameter x_- in eq 1 is the dimensionless coordinate associated with the Q_- vibrational normal coordinate ($Q_- = (\Lambda/k_-)x_-$) having vibrational frequency ν_- and the force constant $k_- = 4\pi^2c^2m\nu_-{}^2$ for the nuclear distortion along this coordinate.[10,12]
(15) It should be noted that the term spin frustration actually describes a system with degenerate spin states. This does not strictly hold for $[4Fe-4S]^{2+}$. In real T_d symmetry the exchange interactions between all four metal centers would be equal. However, the $[4Fe-4S]^{2+}$ clusters do not have T_d symmetry but undergo a compression along a S_4 axis resulting in a D_{2d} symmetry. Thus, the interactions between the metal centers are no longer equal, and the stronger interactions dominate, leading to an irregular spin structure, where spins with antiferromagnetic interaction are aligned parallel due to their weaker coupling as compared to other couplings. There is no longer degeneracy of spin states. Symmetry reduction caused by spin degeneracy has been observed for trinuclear metal clusters in a triangular arrangement and the term magnetic Jahn−Teller effect was introduced.[16−18] Applying this to $[4Fe-4S]^{2+}$ would describe the geometrical distortion as due to the spin degeneracy in tetrahedral symmetry.
(16) Cannon, R. D.; Jayasooriya, U. A.; Wu, R. W.; Arapkoske, S. K.; Stride, J. A.; Nielsen, O. F.; White, R. P.; Kearley, G. J.; Summerfield, D. *J. Am. Chem. Soc.* **1994**, *116*, 11869−11874.
(17) Jayasooriya, U. A.; Cannon, R. D.; Anson, C. E.; Karu, E.; Saad, A. K.; Bourke, J. P.; Kearley, G. J.; White, R. P. *Angew. Chem., Int. Ed.* **1998**, *37*, 317−320.
(18) Wu, R. W.; Poyraz, M.; Sowrey, F. E.; Anson, C. E.; Wocadlo, S.; Powell, A. K.; Jayasooriya, U. A.; Cannon, R. D.; Nakamoto, T.; Katada, M.; Sano, H. *Inorg. Chem.* **1998**, *37*, 1913−1921.
(19) Drüke, S.; Chaudhuri, P.; Pohl, K.; Wieghardt, K.; Ding, X. Q.; Bill, E.; Sawaryn, A.; Trautwein, A. X.; Winkler, H.; Gurman, S. J. *J. Chem. Soc., Chem. Commun.* **1989**, 59−62.
(20) Ding, X. Q.; Bominaar, E. L.; Bill, E.; Winkler, H.; Trautwein, A. X.; Drueke, S.; Chaudhuri, P.; Wieghardt, K. *J. Chem. Phys.* **1990**, *92*, 178−186.
(21) Ding, X. Q.; Bominaar, E. L.; Bill, E.; Winkler, H.; Trautwein, A. X.; Drueke, S.; Chaudhuri, P. H.; Wieghardt, K. *Hyperfine Interactions* **1990**, *53*, 311−315.
(22) Glaser, T.; Beissel, T.; Bill, E.; Weyhermüller, T.; Meyer-Klaucke, W.; Trautwein, A. X.; Wieghardt, K. *J. Am. Chem. Soc.* **1999**, *121*, 2193−2208.
(23) Glaser, T.; Wieghardt, K. In *Spectroscopic Methods in Bioinorganic Chemistry*; Hodgson, K. O., Solomon, E. I., Eds.; ACS Symposium Series; American Chemical Society: Washington, DC, 1998; pp 314−331.
(24) Gamelin, D. R.; Bominaar, E. L.; Kirk, M. L.; Wieghardt, K.; Solomon, E. I. *J. Am. Chem. Soc.* **1996**, *118*, 8085−8097.
(25) Gamelin, D. R.; Bominaar, E. L.; Mathonière, C.; Kirk, M. L.; Wieghardt, K.; Girerd, J. J.; Solomon, E. I. *Inorg. Chem.* **1996**, *35*, 4323−4335.
(26) Glaser, T.; Hedman, B.; Hodgson, K. O.; Solomon, E. I. *Acc. Chem. Res.* **2000**, in press.
(27) Hedman, B.; Hodgson, K. O.; Solomon, E. I. *J. Am. Chem. Soc.* **1990**, *112*, 1643−1645.
(28) Shadle, S. E.; Penner-Hahn, J. E.; Schugar, H. J.; Hedman, B.; Hodgson, K. O.; Solomon, E. I. *J. Am. Chem. Soc.* **1993**, *115*, 767−776.
(29) Shadle, S. E.; Hedman, B.; Hodgson, K. O.; Solomon, E. I. *Inorg. Chem.* **1994**, *33*, 4235−4244.
(30) Shadle, S. E.; Hedman, B.; Hodgson, K. O.; Solomon, E. I. *J. Am. Chem. Soc.* **1995**, *117*, 2259−2272.

K-edges are 1s → np. The K-edge absorption of a ligand bound to a d^9 copper ion exhibits a well-defined preedge feature which is assigned as a ligand 1s → ψ^* transition, where ψ^* is the half-filled, highest-occupied molecular orbital (HOMO) of the Cu^{II} complex. Due to the localized nature of the ligand (L) 1s orbital, this transition can have absorption intensity only if the half-filled HOMO orbital contains a significant component of ligand 3p character as a result of covalency. The intensity of this L 1s → ψ^* transition is given by eq 2 where $\psi^* = (1 - \alpha^2)^{1/2}|\text{Cu } 3d\rangle - \alpha\,|\text{L } 3p\rangle$, and α^2 represents the amount of L 3p character in the HOMO. The observed preedge transition intensity is then the intensity of the pure dipole-allowed L 1s → L 3p transition weighted by α^2.

$$I(\text{L } 1s \rightarrow \psi^*) = \alpha^2 I(\text{L } 1s \rightarrow \text{L } 3p) \qquad (2)$$

Thus, the preedge intensity provides a quantitative estimate of the ligand contribution to the HOMO due to bonding.[27,39] This was used to understand differences in the electronic structure of the blue-copper protein plastocyanin and a model compound.[28]

The preedge feature in d^n metal centers with more than one hole in the d-manifold also corresponds to a transition (or several transitions) from a ligand 1s orbital to unoccupied or partially occupied antibonding orbitals with both metal d- and ligand p-character. These one-electron transitions lead to several many-electron final states due to multiplet effects. Methodology has been developed to analyze these effects for the Cl K-edge preedge intensity in a series of tetrahedral metal tetrachlorides, $[MCl_4]^{n-}$.[30] The results of this methodology can be partitioned into three contributions to the preedge intensity: (i) preedge intensity is proportional to the number of d-holes, that is the number of possible one-electron transitions, (ii) preedge intensity can be redistributed to higher energy through configurational interactions (CI) of allowed parent final states with higher-lying ligand field states of the same symmetry by electron repulsion (this is important for $[Fe^{II}Cl_4]^{2-}$ and $[Co^{II}Cl_4]^{2-}$ where 29 and 16% of the intensity is shifted into a higher-energy state, respectively, which contributes to the edge region rather than the preedge), and (iii) preedge intensity is proportional to the metal−ligand covalency. Thus, taking into account the first two factors, the covalency of compounds with all d^n electron configurations can be analyzed with ligand K-edge XAS. The dipole strength D_0, which is the preedge intensity corrected for CI effects, can be converted to covalency by using eq 3[26]

$$\text{covalency} = \frac{3D_0}{\langle \text{s } |\mathbf{r}|\ \text{p}\rangle^2} \qquad (3)$$

where $\langle \text{s } |\mathbf{r}|\ \text{p}\rangle^2$ is the intensity of a pure ligand 1s → 3p transition. The covalency defined in this way is the sum of the individual covalencies per orbital and involves the summation over all un- or half-occupied orbitals.[40] To use eq 3, reference compounds with known covalencies are needed. For Cl K-edges, the known Cu−Cl covalency (7.5% per bond) of D_{2d}-$[Cu^{II}Cl_4]^-$ is used.[29,30] The following covalencies per metal−ligand bond were determined for the metal tetrachlorides: 7.5% (Cu^{II}, D_{2d}), 10.7% (Cu^{II}, D_{4h}), 6.1% (Ni^{II}), 7.1% (Co^{II}), 8.6% (Fe^{II}), and 21.5% (Fe^{III}), which correlate to calculated results. For S K-edges, references for thiolate and sulfide have been established by independent spectroscopies: plastocyanin (38% Cu−thiolate covalency)[28] and the infinitive chain compound $CsFe^{III}S_2$ (55.5% Fe−sulfide covalency).[34]

The correlation between S preedge intensity and covalency has also been developed for an analogous $[M(SR)_4]^{2-}$ series, where M = Ni^{II}, Co^{II}, Fe^{II}, and Mn^{II}.[31] The anisotropy of the thiolate p-orbitals in bonding to the metal was evaluated. A study of ferrous and ferric model complexes and a series of rubredoxins has also been performed.[33] In that study, it was established that the ferric model complex had a S-K preedge feature that was similar in shape and energy to that of the proteins. Finally, we have applied this methodology to the analysis of 2Fe−2S dimer complexes in which two types of sulfur ligands are present: terminal thiolate and bridging sulfide ligands.[34] Due to differences in the effective nuclear charge of the thiolate and the sulfide, their preedge features could be resolved allowing for evaluation of the individual covalencies. It was established that the sulfide ligand is 2−3 times more covalent than the thiolate ligand. Covalencies are reported as a per bond property taking into account the occurrence of several ligands of the same type in one molecule and the bridging mode of the ligand.

Here, our ligand K-edge XAS studies on Fe−S clusters are extended to investigate the electronic structure of tetrameric Fe−S model complexes. In comparison to the results on dimeric Fe−S clusters, the differences in iron-ligand covalencies and in effective nuclear charges on the iron centers are established. A relationship, which describes the dependence of the superexchange coupling constant on the covalency of bridging ligand, is derived and used to evaluate the change in superexchange between the metal centers in dimeric and tetrameric Fe−S clusters. In conjunction with changes in double exchange and vibronic coupling contributions, a quantitative description of the localized mixed-valence ground state in the dimer and the delocalized mixed-valence ground state of the dimer subsite in the tetramer is obtained. This first application of the ligand K-edge XAS methodology to tetrameric Fe−S clusters also forms the basis for studies of the $[Fe_4S_4]^{2+}$ state in HiPIP and in the 4Fe ferredoxin to obtain insight into the H-bonding and the ~1 V difference in their reduction potentials,[37] and of the different oxidation states of the tetrameric models and protein sites to define differences in covalency related to electronic relaxation.[38]

(31) Rose Williams, K.; Hedman, B.; Hodgson, K. O.; Solomon, E. I. *Inorg. Chim. Acta* **1997**, *263*, 315−321.
(32) Rose Williams, K.; Gamelin, D. R.; LaCroix, L. B.; Houser, R. P.; Tolman, W. B.; Mulder, T. C.; deVries, S.; Hedman, B.; Hodgson, K. O.; Solomon, E. I. *J. Am. Chem. Soc.* **1997**, *119*, 613−614.
(33) Rose, K.; Shadle, S. E.; Eidsness, M. K.; Kurtz, D. M., Jr; Scott, R. A.; Hedman, B.; Hodgson, K. O.; Solomon, E. I. *J. Am. Chem. Soc.* **1998**, *120*, 10743−10747.
(34) Rose, K.; Shadle, S. E.; Glaser, T.; de Vries, S.; Cherepanow, A.; Canters, G. W.; Hedman, B.; Hodgson, K. O.; Solomon, E. I. *J. Am. Chem. Soc.* **1999**, *121*, 2353−2363.
(35) Izumi, Y.; Glaser, T.; Rose, K.; McMaster, J.; Basu, P.; Enemark, J. H.; Hedman, B.; Hodgson, K. O.; Solomon, E. I. *J. Am. Chem. Soc.* **1999**, *121*, 10035−10046.
(36) Neese, F.; Hedman, B.; Hodgson, K. O.; Solomon, E. I. *Inorg. Chem.* **1999**, *38*, 4854−4860.
(37) Glaser, T.; Bertini, I.; Moura, J. J. G.; Hedman, B.; Hodgson, K. O.; Solomon, E. I. Submitted for publication.
(38) Szilagyi, R., Glaser, T.; Holm, R. H.; Moura, J. J. G.; Bertini, I.; Hedman, B.; Hodgson, K. O.; Solomon, E. I. Manuscript in preparation.
(39) From the experimental lack of shake-up satellites and calculations[36] these ligand core transitions do not show significant electronic relaxation effects on the intensity/covalency analysis. This is because the mechanism of relaxation would involve valence charge compensation of the core hole produced. This would require metal-to-ligand CT which is not an available channel with donor ligands such as chloride, thiolate, and sulfide.

(40) Here we use the term covalency in the sense of the Mulliken, NBO, or AIM spin density, where we probe this experimentally through edge transitions to the spin-down unoccupied counterparts of the occupied spin-up orbitals.

Experimental Section

Sample Preparation. The model complexes $[Ph_4P]_2[Fe_4S_4(SEt)_4]$,[41] $[Et_4N]_2[Fe_4S_4(Smes)_4]$,[42] $[Et_4N]_2[Fe_4S_4(SBz)_4]$,[43] $[n\text{-}Bu_4N]_2[Fe_4S_4(SPh)_4]$,[44] $[Me_4N]_2[Fe_4Se_4(SPh)_4]$,[45] $[n\text{-}Bu_4N]_2[Fe_4S_4Cl_4]$,[46] $[Et_4N]_2[Fe_2S_2Cl_4]$,[47] $[Et_4N]_2[Fe_2Se_2(SPh)_4]$,[48] $[Et_4N]_2[Fe(SPh)_4]$,[49] and $[Et_4N][Fe(SPh)_4]$[50] were prepared according to the referenced procedures.

X-ray Absorption Spectroscopy Measurements. XAS data were measured at the Stanford Synchrotron Radiation Laboratory using the 54-pole wiggler beam line 6−2. Details of the experimental configuration for low energy studies have been described in an earlier publication.[51] The preparation of the K-edge XAS samples, details of the measurement, data reduction, fitting procedure, and error source and analysis follow the previously published protocol.[29−35]

Electronic Structure Calculations. For the VBCI calculations, the commercial software "Mathcad Professional" was used. Density functional calculations were performed on IBM 3BT-RS/6000 work stations and a SGI Origin 2000 using the Amsterdam Density Functional (ADF) program version 2.0.1 and ADF 1999, respectively, developed by Baerends et al.[52,53] A triple-ζ Slater-type orbital basis set (ADF basis set IV) with a single polarization function at the local density approximation of Vosko, Wilk, and Nusair[54] and the nonlocal gradient corrections of Becke[55] and Perdew[56] were employed. Complete coordinates of all models presented in the text are included in the Supporting Information. The choice in bond distances and bond angles followed the approach of Noodleman and co-workers.[13,57−60] The calculation on the binuclear Fe−S clusters were performed in the broken symmetry and high-spin state.[61] The geometry for the broken symmetry state calculation was performed in C_{2v}, whereas the geometry for the high-spin calculation was symmetrized to D_{2h} symmetry.[59] The negatively charged molecules were charge neutralized by placing point charges at a distance approximated by the position of the positive counterion in the crystal structures.[62] Comparison of calculations performed with and without point charges gives only minor differences in the MO coefficients and relative orbital energies.

(41) Hagen, K. S.; Watson, A. D.; Holm, R. H. *J. Am. Chem. Soc.* **1983**, *105*, 3905−3913.
(42) Zhou, J.; Scott, M. J.; Hu, Z. G.; Peng, G.; Münck, E.; Holm, R. H. *J. Am. Chem. Soc.* **1992**, *114*, 10843−10854.
(43) Averill, B. A.; Herskovitz, T.; Holm, R. H.; Ibers, J. A. *J. Am. Chem. Soc.* **1973**, *95*, 3523−3534.
(44) Hagen, K. S.; Berg, J. M.; Holm, R. H. *Inorg. Chim. Acta* **1980**, *45*, L17−L18.
(45) Bobrik, M. A.; Laskowski, E. J.; Johnson, R. W.; Gillum, W. O.; Berg, J. M.; Hodgson, K. O.; Holm, R. H. *Inorg. Chem.* **1978**, *17*, 1402−1410.
(46) Wong, G. B.; Bobrik, M. A.; Holm, R. H. *Inorg. Chem.* **1978**, *17*, 578−584.
(47) Do, Y.; Simhon, E. D.; Holm, R. H. *Inorg. Chem.* **1983**, *22*, 3809−3812.
(48) Reynolds, J. G.; Holm, R. H. *Inorg. Chem.* **1980**, *19*, 3257−3260.
(49) Holah, D. G.; Coucouvanis, D. J. *J. Am. Chem. Soc.* **1975**, *97*, 6917−6919.
(50) Koch, S. A.; Maelia, L. E.; Millar, M. J. *J. Am. Chem. Soc.* **1983**, *105*, 5944−5945.
(51) Hedman, B.; Frank, P.; Gheller, S. F.; Roe, A. L.; Newton, W. E.; Hodgson, K. O. *J. Am. Chem. Soc.* **1988**, *110*, 3798−3805.
(52) Baerends, E. J.; Ellis, D. E.; Ros, P. *Chem. Phys.* **1973**, *2*, 41−51.
(53) te Velde, G.; Baerends, E. J. *Int. J. Comput. Phys.* **1992**, *99*, 84−98.
(54) Vosko, S. H.; Wilk, L.; Nusair, M. *Can. J. Phys.* **1980**, *58*, 1200−1211.
(55) Becke, A. D. *J. Chem. Phys.* **1986**, *84*, 4524−4529.
(56) Perdew, J. P. *Phys. Rev. B* **1986**, *33*, 8822−8824.
(57) Norman, J. G.; Ryan, P. B.; Noodleman, L. *J. Am. Chem. Soc.* **1980**, *102*, 4279−4282.
(58) Noodleman, L.; Norman, J. G.; Osborne, J. H.; Aizman, A.; Case, D. A. *J. Am. Chem. Soc.* **1985**, *107*, 3418−3426.
(59) Mouesca, J. M.; Chen, J. L.; Noodleman, L.; Bashford, D.; Case, D. A. *J. Am. Chem. Soc.* **1994**, *116*, 11898−11914.
(60) Li, J.; Nelson, M. R.; Peng, C. Y.; Bashford, D.; Noodleman, L. *J. Phys. Chem. A* **1998**, *102*, 6311−6324.
(61) Noodleman, L. *J. Chem. Phys.* **1981**, *74*, 5737−5743.
(62) Atanasov, M.; Brunold, T. C.; Güdel, H. U.; Daul, C. *Inorg. Chem.* **1998**, *37*, 4589−4602.

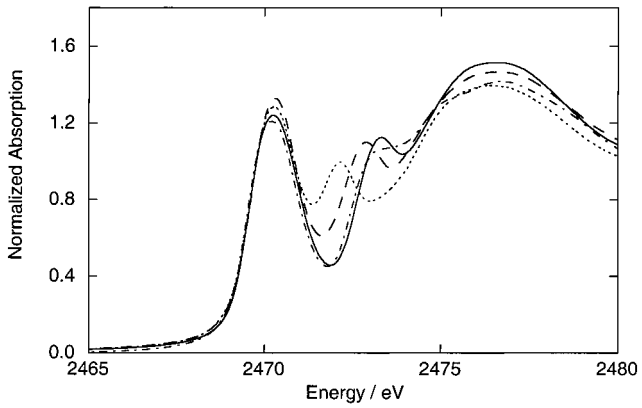

Figure 1. Normalized S K-edge spectra of tetrameric Fe−S clusters: $[n\text{-}Bu_4N]_2[Fe_4S_4(SPh)_4]$ (—), $[Ph_4P]_2[Fe_4S_4(SEt)_4]$ (− − −), $[Et_4N]_2[Fe_4S_4(Smes)_4]$ (−•−•−•), and $[Et_4N]_2[Fe_4S_4(SBz)_4]$ (•••).

Table 1. Energies and Intensities for S and Cl K-edge XAS Spectra of Tetrameric Fe−S Clusters

	preedge energy[a]	preedge intensity[b]	thiolate peak energy[c]	rising edge inflection point[d]
$[Fe_4S_4(SPh)_4]^{2-}$	2470.2	1.80 ± 0.06	2473.3	2472.5
$[Fe_4S_4(SEt)_4]^{2-}$	2470.3	1.96 ± 0.07	2472.9	2472.2
$[Fe_4S_4(SBz)_4]^{2-}$	2470.3	1.72 ± 0.09	2472.1	2471.7
$[Fe_4S_4(Smes)_4]^{2-}$	2470.2	1.72 ± 0.08	2473.3	2472.4
$[Fe_4Se_4(SPh)_4]^{2-}$	2470.6	0.94 ± 0.03	2473.2	2472.5
$[Fe_4S_4Cl_4]^{2-}$	2470.0	2.57 ± 0.22	—	2474.2
$[Fe_4S_4Cl_4]^{2-}$ [e]	2821.7[e]	1.03 ± 0.09[e]	—	2825.4[e]

[a] Preedge energies from maximum of the experimental data. [b] Total preedge intensities after background subtraction. [c] Thiolate edge peak energy from the experimental maximum. [d] Rising edge inflection point is obtained from the highest-energy maximum of the first derivative in the rising-edge region. [e] Cl K-edge.

Results

The S K-edge XAS spectra of the tetrameric Fe−S clusters $[n\text{-}Bu_4N]_2[Fe_4S_4(SPh)_4]$, $[Ph_4P]_2[Fe_4S_4(SEt)_4]$, $[Et_4N]_2[Fe_4S_4(Smes)_4]$, and $[Et_4N]_2[Fe_4S_4(SBz)_4]$ are shown in Figure 1. The spectra consist of two regions, the edge region and the preedge region. In the edge region (∼2472−2475 eV), the spectra exhibit a peak of varying energy depending on the nature of the organic group R (Table 1, third column). This transition is not assigned to the preedge, because it also appears in the free ligands. The origin of this transition can be derived from the comparison in Figure 2 between the S K-edge spectra of complexes having only sulfide S^{2-} (solid lines) and of complexes having only thiophenolates PhS^- (dashed lines) as a source of sulfur. The compounds with sulfides only show a rising edge at ∼2474 eV, while the thiophenolate compounds all exhibit an intense edge peak at lower energy (∼2472.2 eV), which is absent in the sulfide spectra. This lower energy peak is also present in the spectra of compounds with only benzylic or aliphatic thiolates. Aliphatic edge features occur at ∼2472.9 eV and benzylic edge peaks occur to lower energy at ∼2472.0 eV. These observations lead to the assignment of the intense thiolate edge-features as S 1s → σ^*(C−S) transitions. The energies and intensities therefore strongly depend on the type of S−C bond present in the thiolate. The presence of the thiolate S 1s → σ^*(C−S) transition complicates the determination of the main edge-jump position which is a measure of the ligand 1s binding energy. However, the energy differences between the rising edge inflection points of compounds with the same ligand are still a good measure for the trends in the ligand core binding energies.

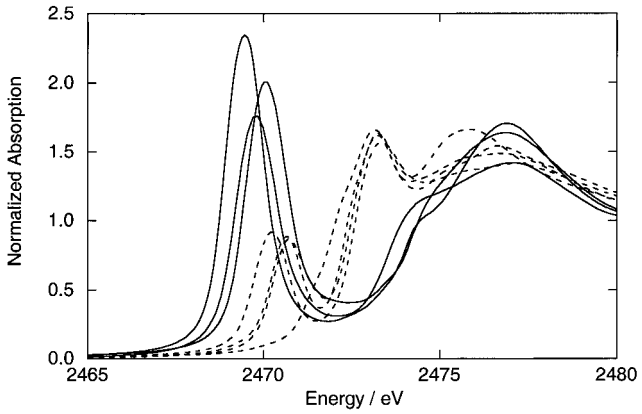

Figure 2. Normalized S K-edge spectra of complexes containing only sulfides (solid lines) and only thiolates (dashed lines). The sulfide complexes are: $[n\text{-}Bu_4N]_2[Fe_4S_4Cl_4]$, $[Et_4N]_2[Fe_2S_2Cl_4]$, and $CsFeS_2$ and the thiolate complexes are: $[Me_4N]_2[Fe_4Se_4(SPh)_4]$, $[Et_4N]_2[Fe_2Se_2(SPh)_4]$, $[Et_4N]_2[Fe(SPh)_4]$, and $[Et_4N][Fe(SPh)_4]$.

In the preedge region, all spectra shown in Figure 1 exhibit an intense preedge feature (~2470.2−2470.3 eV) with similar overall intensity. This feature is the superposition of transitions originating from the bridging sulfides and the terminal thiolates. This is corroborated by the S K-edge XAS spectra of $[Me_4N]_2[Fe_4Se_4(SPh)_4]$ and $[n\text{-}Bu_4N]_2[Fe_4S_4Cl_4]$ (Figure 3a). The preedge feature of the selenide-substituted complex $[Me_4N]_2[Fe_4Se_4(SPh)_4]$, which contains only terminal thiolate sulfurs, is at 2470.6 eV, whereas the preedge feature of the chloride-substituted complex $[n\text{-}Bu_4N]_2[Fe_4S_4Cl_4]$, which contains only bridging sulfides, is at 2470.0 eV (Table 1, first column). The appropriately renormalized[63] sum of these two spectra models very well the S K-edge spectrum of $[n\text{-}Bu_4N]_2[Fe_4S_4(SPh)_4]$, which has contributions from both types of sulfur ligands (dotted line in Figure 3a). The energy separation between the sulfide and the thiolate preedge transitions reflects the lower core binding energy (lower effective nuclear charge) of the sulfide ligand. Comparison to the S K-edge spectrum of the dimeric Fe−S cluster $[Et_4N]_2[Fe_2S_2(SPh)_4]$[34] (Figure 3b) shows a larger energy splitting of the transitions for the dimer (1.2 eV) than for the tetramer (0.7 eV). This decreased energy separation in the tetramer is mainly due to a 0.6 eV shift of the sulfide preedge feature to higher energy, whereas the thiolate peak energy is essentially unchanged. The trend in the preedge energies of the complexes with terminal chloride ligands is consistent with that observed for the complexes with terminal thiolate ligands (Figure S1, Supporting Information). The Cl K-edge spectrum of $[n\text{-}Bu_4N]_2[Fe_4S_4Cl_4]$ exhibits only a small shift of 0.2 eV in the preedge energy compared to that of $[Et_4N]_2[Fe_2S_2Cl_4]$.

The intensities of the preedge features were determined by peak fitting in order to calculate the covalencies. There are two modifications to the preedge fitting procedure relative to earlier publications.[29−31,34] An experimental estimate for the background of the rising edge was obtained from spectra of free ligands and from $[Mn^{II}(S\text{−}Ph\text{-}2\text{-}Ph)_4]^{2-}$, in which the preedge is shifted into the edge due to its low effective nuclear charge.[31] These experimental estimates for the background result in more accurate values for the preedge intensities with less error from the fitting procedure. Additionally, the line widths of the Voigt lines (1:1 ratio) were allowed to float independently, because the preedge of ferric and ferrous complexes consists of several transitions, which are not experimentally resolved. Thus, the Voigt lines do not represent single transitions but the overall line shape due to multiple unresolved transitions. The intensities obtained in this way are reported in Table 1. The intensities given for the compounds with both terminal thiolates and bridging sulfides are not separated into individual contributions due to their unresolved preedge features.

(63) Renormalization is defined as: ligand preedge intensity of one transition multiplied by the total number of absorbers in the molecule divided by the number of ligand atoms contributing to the respective preedge transition. This procedure yields the preedge intensity per absorbing atom. For a bridging atom, this renormalized intensity has to be divided by the number of bound metals to obtain the intensity per bond.

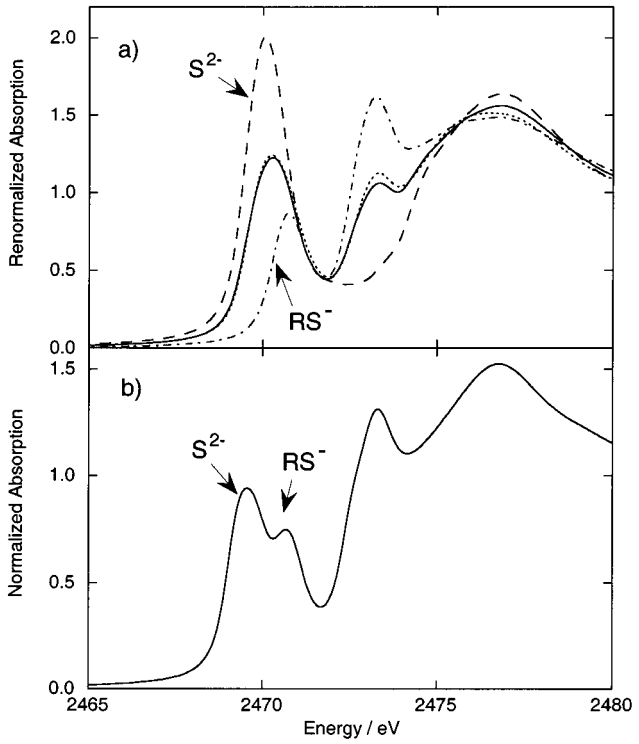

Figure 3. (a) Normalized S K-edge spectra of $[Me_4N]_2[Fe_4Se_4(SPh)_4]$ (−•−•−•) showing only features due to terminal thiolates, and of $[n\text{-}Bu_4N]_2[Fe_4S_4Cl_4]$ (− − −) showing only features due to bridging sulfides. The addition of these S K-edge spectra (——) models well the S K-edge spectrum of $[n\text{-}Bu_4N]_2[Fe_4S_4(SPh)_4]$ (···), containing both terminal thiolates and bridging sulfides. The renormalized addition spectrum was obtained by adding 4/8 of the normalized S K-edge spectrum of $[n\text{-}Bu_4N]_2[Fe_4S_4Cl_4]$ and 4/8 of the normalized S K-edge spectrum of $[Me_4N]_2[Fe_4Se_4(SPh)_4]$. (b) Normalized S K-edge spectrum of $[Et_4N]_2[Fe_2S_2(SPh)_4]$ (adapted from ref 34) demonstrating the decreased energy separation of the preedge features of thiolate and sulfide in the 4Fe−4S tetramer as compared to that of the 2Fe−2S dimer.

Analysis

To understand the localization of the excess electron in the mixed-valence dimeric Fe−S clusters as compared to the delocalization of the excess electron over a pair of iron centers in the tetrameric Fe−S clusters, a quantitative comparison of the bonding interactions between the iron sites was performed using ligand K-edge XAS. The dimerization of two dimers to form a tetramer, with loss of one thiolate per iron, changes the nature of the bridging ligand from a μ_2-bridging sulfide to a μ_3-bridging sulfide (Scheme 2). The comparison of the previously measured $[Fe^{III}{}_2S_2]^{2+}$ dimers and the preedge of the $[Fe^{2.5}{}_4S_4]^{2+}$ clusters experimentally determined here (Figure 4) is not straightforward because two properties of the cluster have changed: *i)* the nature of the bridging ligand (μ_2 to μ_3), and *ii)*

Scheme 2

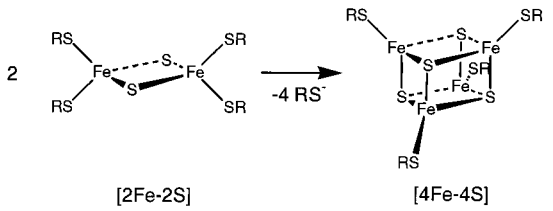

the oxidation state (localized diferric to a delocalized $2Fe^{2.5}$ subdimer). The appropriate comparison for the interactions between the metal sites in the dimer and the tetramer would be with a delocalized dimeric unit $Fe^{2.5}{}_2$, as the only change on going from the dimer to the tetramer would be the bridging mode of the sulfide. In section I of this Analysis, the derivation of the transition energies and intensities of the ligand K-edge spectra of the hypothetical mixed-valence delocalized dimer $[Fe^{2.5}{}_2S_2X_4]^{3-}$ ($X = Cl^-$, RS^-) unit is described and the covalencies of its ligands are compared to those of the delocalized dimer subsite in the mixed-valence tetramer. In section II, the dependence of the phenomenological superexchange coupling constant J on the covalency of the bridging ligand determined in section I is derived.

I. Quantitative Comparison between 4Fe−4S and 2Fe−2S. The principal strategy used to determine the properties (transition energies and intensities) of a hypothetical mixed-valence delocalized dimer $[Fe^{2.5}{}_2S_2X_4]^{3-}$ is to first derive the properties of a hypothetical diferrous dimer and then to average the properties of the hypothetical diferrous and the measured diferric complexes. This latter approach treats the properties of a fully delocalized dimer as the mean of the properties of the ferrous and the ferric site.[64] The properties of the hypothetical diferrous unit are estimated on the basis of experimentally determined chemical shifts from spectra of monomeric ferrous and ferric compounds and of the μ_2-sulfide-bridged diferric complex. The energies of the diferrous dimer are based on the energies of the ferrous monomer, which are corrected for the effect of replacing two terminal ligands with two μ_2-bridging sulfides. The experimentally observed energy shift on going from the ferric monomer complex to the ferric dimer complex gives an estimate for this correction (Scheme 3). The transition intensity of the hypothetical diferrous dimer is based on the intensity of the diferric compound which is scaled by the ratio of the intensities of the monomeric ferrous and ferric compounds to account for the change in oxidation state. For derivation of the properties of the bridging sulfide ligand in the diferrous dimer, the spectral data of the Fe^{II}−sulfide bond in reduced ferredoxin are used.[65] These data are corrected for the presence of the adjacent ferric site in reduced ferredoxin.

Most of the values that are needed to define the hypothetical diferrous dimer are available from measured data. Some features have been estimated from density functional calculations; however, it should be emphasized that these calculations have only been used-to-establish ratios, which have been evaluated by comparison with experiment. First the properties of the terminal chloride and thiolate ligands are analyzed and then the properties of the bridging sulfides.

A. Terminal Ligands: Chlorides and Thiolates. This section describes how the energy and intensity of the K preedge features of the terminal ligands for a hypothetical delocalized mixed-valence dimer $[Fe^{2.5}{}_2S_2X_4]^{3-}$ ($X = Cl^-$, RS^-) were derived. These properties are the average of those of the ferric

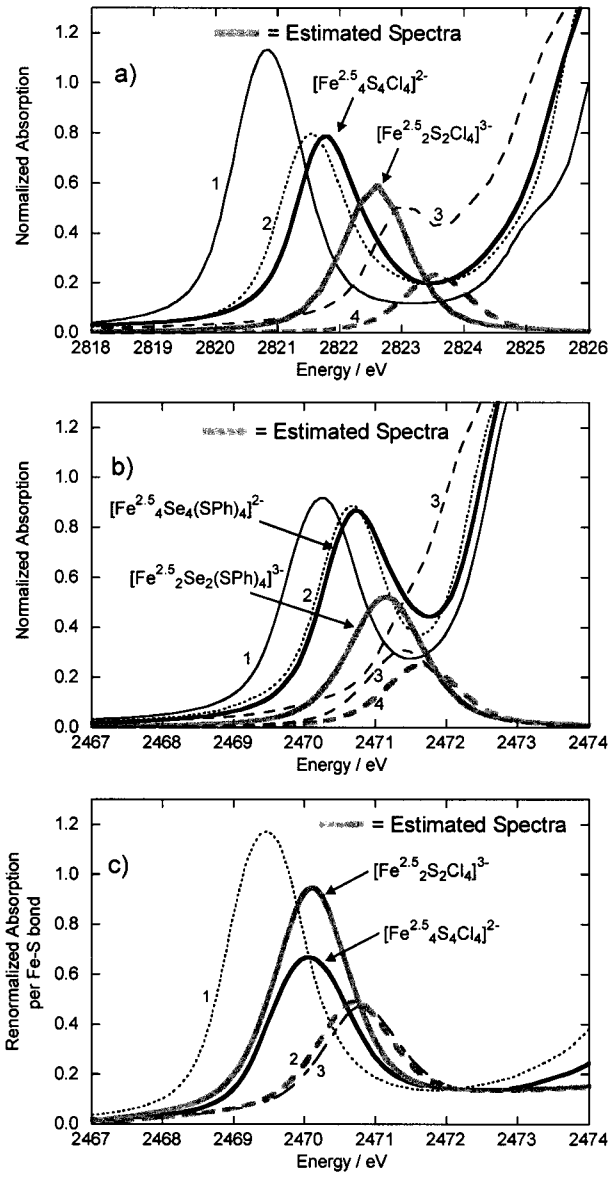

Figure 4. Chemical shifts observed in the preedge spectra of Fe−S compounds: (a) chlorides, (b) thiolates, and (c) sulfides. (a) Comparison of normalized measured Cl K-edge spectra of $[Et_4N][Fe^{III}Cl_4]$ (solid, 1), $[Et_4N]_2[Fe^{II}Cl_4]$ (dashed, 3), $[Et_4N]_2[Fe^{III}{}_2S_2Cl_4]$ (dotted, 2), $[Et_4N]_2[Fe^{2.5}{}_4S_4Cl_4]$ (bold solid), and estimated preedges of $[Fe^{2.5}{}_2S_2Cl_4]^{3-}$ (grey solid) and $[Fe^{II}{}_2S_2Cl_4]^{4-}$ (grey dashed, 4). (b) Comparison of normalized measured S K-edge spectra of $[Et_4N][Fe^{III}(SPh)_4]$ (solid, 1), $[Et_4N]_2[Fe^{II}(SPh)_4]$ (dashed, 3, representative fit to the preedge), $[Et_4N]_2[Fe^{III}{}_2Se_2(SPh)_4]$ (dotted, 2), $[Me_4N]_2[Fe^{2.5}{}_4Se_4(SPh)_4]$ (bold solid), and estimated preedges of $[Fe^{2.5}{}_2Se_2(SPh)_4]^{3-}$ (grey solid) and $[Fe^{II}{}_2Se_2(SPh)_4]^{4-}$ (grey dashed, 4). (c) Comparison between the normalized measured S K-edge spectra of $[Et_4N]_2[Fe^{III}{}_2S_2Cl_4]$ (dotted, 1) and $[Et_4N]_2[Fe^{2.5}{}_4S_4Cl_4]$ (bold solid) and the estimated preedges of $[Fe^{2.5}{}_2S_2Cl_4]^{3-}$ (grey solid) and $[Fe^{II}{}_2S_2Cl_4]^{4-}$ (grey dashed, 2). The preedge feature of the Fe^{II}−sulfide from reduced FdI is included (dashed-dotted, 3) as reference. *Note that the intensity plotted is on a per-bond basis.* To provide a fair visual comparison, a linear background is added to the estimated peaks and the peak of FdI. Note also that the measured preedge feature of the terminal chloride and thiolate ligands in the delocalized mixed-valence tetramer is *more* intense and at lower energy than that of the hypothetical delocalized mixed-valence dimer, whereas the measured preedge feature resulting from the bridging sulfide ligands in the delocalized mixed-valence tetramer is *less* intense than that of the hypothetical delocalized mixed-valence dimer.

(64) Perrée-Fauvet, M.; Gaudemer, A.; Bonvoisin, J.; Girerd, J.-J.; Boucly-Goester, C.; Boucly, P. *Inorg. Chem.* **1989**, *28*, 3533−3538.

(65) Anxolabéhère-Mallart, E.; Glaser, T.; Frank, P.; Hedman, B.; Aliverti, A.; Zanetti, G.; Hodgson, K. O.; Solomon, E. I. Manuscript in preparation.

Scheme 3

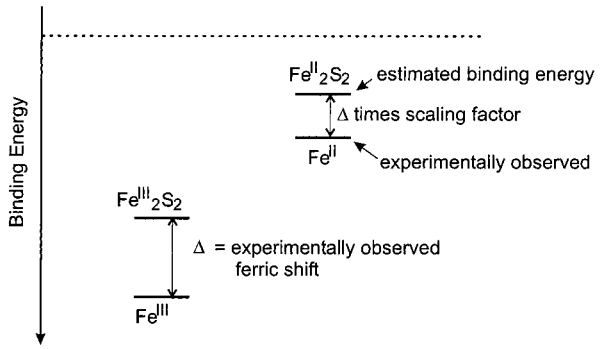

$[Fe^{III}{}_2S_2X_4]^{2-}$ and the ferrous $[Fe^{II}{}_2S_2X_4]^{4-}$ dimers.[64] The preedge of the ferric dimer is experimentally observed (Figure 4a and b, dotted spectra), while the energy and then the intensity of the diferrous dimer is estimated as described below.

The preedge energy is the difference between the rising edge inflection point and the relative d-manifold binding energy.[66] The determination of the rising edge inflection point for the hypothetical diferrous dimer $[Fe^{II}{}_2S_2Cl_4]^{4-}$ is based on the experimentally determined rising edge inflection point of $[Fe^{II}Cl_4]^{2-}$ (Table 2). This energy has to be corrected for the change in the ligand environment, i.e. substituting two chlorides in $[Fe^{II}Cl_4]^{2-}$ by two μ_2-bridging sulfides to give $[Fe^{II}{}_2S_2Cl_4]^{4-}$. The correction is based on the experimentally observed energy shift in the rising edge inflection point on going from $[Fe^{III}Cl_4]^{-}$ to $[Fe^{III}{}_2S_2Cl_4]^{2-}$, which has the same change in the ligand sphere. The rising edge inflection point of $[Fe^{III}{}_2S_2Cl_4]^{2-}$ is 0.4 eV lower in energy (Table 2).[67] The energy shift on going from the ferrous monomer to the ferrous dimer is smaller, because less charge compensation is expected in the more electron-rich ferrous sites. To account for this decreased energy shift in the ferrous compounds, density functional calculations for the thiolate complexes were used to determine a scaling factor for the ferrous relative to the ferric energy shifts (Scheme 3). The organic group in the thiolate compounds provides an internal energy reference which is not available in the chloride compounds. This procedure[68] gives a scaling factor for ferrous-to-ferric energy shifts of 0.57. Applying this factor to the energy difference of the rising edge inflection points for the ferric chloride complexes and adding the result to the observed rising edge inflection point of $[Fe^{II}Cl_4]^{2-}$ gives a rising edge inflection point for the hypothetical diferrous dimer $[Fe^{II}{}_2S_2Cl_4]^{4-}$ of 2824.8 eV (Table 2).

An analogous approach was used to obtain the relative d-manifold binding energy of the hypothetical diferrous dimer $[Fe^{II}{}_2S_2Cl_4]^{4-}$. Starting from the relative d-manifold binding energy of the ferrous monomer $[Fe^{II}Cl_4]^{2-}$ and adding the shift in d-manifold binding energy on going from $[Fe^{III}Cl_4]^{-}$ to $[Fe^{III}{}_2S_2Cl_4]^{2-}$ (scaled down by the ferrous-to-ferric energy shift ratio) leads to the relative d-manifold binding energy of $[Fe^{II}{}_2S_2Cl_4]^{4-}$. The energy shift in the ferric chlorides is 1.2 eV (Table 2) due to the increased total charge donation in the dimer (quantified by 166% total covalency in the dimer[33] and 86% in the monomer[32]). Scaling by 0.57 gives the ferrous shift, which is added to the relative d-manifold binding energy of $[Fe^{II}Cl_4]^{2-}$ to give a binding energy for the hypothetical $[Fe^{II}{}_2S_2Cl_4]^{4-}$ of 1.2 eV. The preedge energy of the hypothetical $[Fe^{II}{}_2S_2Cl_4]^{4-}$ is then the difference of the rising edge inflection point and the relative d-manifold binding energy. This gives a value of 2823.6 eV.[69]

The analogous procedure for the terminal thiolate ligands of the hypothetical dimer $[Fe^{II}{}_2Se_2(SPh)_4]^{4-}$ using the ferrous monomer $[Fe^{II}(SPh)_4]^{2-}$, the ferric monomer $[Fe^{III}(SPh)_4]^{-}$, and the ferric dimer $[Fe^{III}{}_2Se_2(SPh)_4]^{2-}$ gives the rising edge inflection point of $[Fe^{II}{}_2Se_2(SPh)_4]^{4-}$ at 2472.8 eV and the d-manifold binding energy at 1.1 eV. The difference between these two values gives the energy of the preedge in the hypothetical ferrous dimer $[Fe^{II}{}_2Se_2(SPh)_4]^{4-}$ at 2471.7 eV (Table 3).

The next step is the determination of the preedge intensity of the hypothetical ferrous dimer $[Fe^{II}{}_2S_2Cl_4]^{4-}$ based on the measured intensity of the ferric dimer $[Fe^{III}{}_2S_2Cl_4]^{2-}$. To account for the change in oxidation state, this intensity was scaled by the experimental ferrous-to-ferric intensity ratio which was obtained from the Cl K-edge spectra of $[Fe^{II}Cl_4]^{2-}$ and $[Fe^{III}Cl_4]^{-}$ (Table 2). To calculate this intensity ratio the dipole strength for $[Fe^{II}Cl_4]^{2-}$ must be used. The dipole strength already includes the correction for preedge intensity shifted to higher energy by CI mixing (vide supra).[70] Using dipole strengths of 0.60 for $[Fe^{II}Cl_4]^{2-}$ and 1.51 for $[Fe^{III}Cl_4]^{-}$ gives an experimental ferrous-to-ferric ratio of 0.40. Applying this experimental ratio to the dipole strength of $[Fe^{III}{}_2S_2Cl_4]^{2-}$ gives an estimate for the dipole strength of $[Fe^{II}{}_2S_2Cl_4]^{4-}$ of 0.43. Because the ferrous monomer loses some preedge intensity by CI mixing into higher multiplet states, the dipole strength of the ferrous dimer has to be corrected for this intensity shifted to higher energy. Using the same correction factor as in the monomer yields a preedge intensity of 0.30 for $[Fe^{II}{}_2S_2Cl_4]^{4-}$. An estimated preedge for $[Fe^{II}{}_2S_2Cl_4]^{4-}$ at 2823.6 eV with an intensity of 0.30 is included as spectrum 4 in Figure 4a.

The preedge dipole strength of the terminal thiolate ligands of the hypothetical ferrous dimer $[Fe^{II}{}_2Se_2(SPh)_4]^{4-}$ is based on the measured dipole strengths of the ferric dimer $[Fe^{III}{}_2Se_2-$

(66) Note that the energy of the edge, which is the onset of transitions into the continuum, is not experimentally defined because it is not resolved but masked by other transitions. The best estimate is the highest energy maximum in the first derivative since the edge-transitions are at lower energy and do not contribute significantly to the first derivative. However, by using the same reference point (the rising edge inflection point) differences between binding energies are absolute.

(67) This energy difference is an estimate for the difference in Cl 1s binding energies for these two complexes. The stronger sulfide donors lead to less charge donation from the remaining chloride ligands. This is quantified by the decrease in Cl covalency from 22% in the monomer to 15% in the dimer.[34] The reduced charge donation of the chloride ligands leads to a lower effective nuclear charge on the chlorides and therefore to the reduced binding energy.

(68) The ferrous-to-ferric energy shift ratio was determined by using the calculated electronic structures of $[Fe^{II}(SMe)_4]^{2-}$, $[Fe^{III}(SMe)_4]^{-}$, $[Fe^{II}{}_2S_2(SMe)_4]$,$^{4-}$ and $[Fe^{III}{}_2S_2(SMe)_4]^{2-}$. By using a C−H bond of the methylthiolate as internal energy reference, the relative d-orbital energies were determined and converted to a ferrous-to-ferric energy shift ratio. The energy level diagrams of the unoccupied spin-down (or β) d-orbitals and one of the C−H bonds for these complexes are shown in Figure S2. An averaged d-orbital energy (unoccupied spin-down) is calculated for each complex by weighting each d-orbital energy with its thiolate MO character. The energy difference between this weighted energy and the energy of the internal C−H bond yields the following thiolate-contribution weighted d-orbital energies: 7.654 eV in $[Fe^{III}(SMe)_4]^{-}$, 8.166 eV in $[Fe^{III}{}_2S_2(SMe)_4]^{2-}$, 8.450 eV in $[Fe^{II}(SMe)_4]^{2-}$, and 8.743 eV in $[Fe^{II}{}_2S_2(SMe)_4]$.$^{4-}$ Substitution of two thiolates by two μ_2-bridging sulfides, i.e. on going from $[Fe^{III}(SMe)_4]^{-}$ to $[Fe^{III}{}_2S_2(SMe)_4]^{2-}$, leads to a shift in the thiolate contribution weighted d-orbital energy of 0.512 eV. For the analogous ferrous complexes, this shift is 0.293 eV. The ratio of these two values (0.57) is the ratio of the ferrous-to-ferric energy difference shift associated with substitution of two terminal ligands by two μ_2-bridging sulfides.

(69) It should be noted that the preedge energy of the diferrous dimer $[Fe^{II}{}_2S_2Cl_4]^{4-}$ could equivalently be calculated by adding to the preedge energy of the ferrous monomer $[Fe^{II}Cl_4]^{2-}$ the difference of the preedge energies of ferric dimer $[Fe^{III}{}_2S_2Cl_4]^{2-}$ and the ferric monomer $[Fe^{III}Cl_4]^{-}$ rescaled by the ferrous-to-ferric energy shift ratio.

(70) Note that the computation of the dipole strength (D_0) from the observed preedge intensity and the configuration interaction correction factor in Table 8 of ref 30 was incorrect. The correct dipole strength is 0.604.

Table 2. Analysis of the Cl K-edges of Fe−S Clusters and Relevant Reference Compounds

	rising edge inflection point[a]	preedge energy[b]	relative d-manifold energy shift[c]	preedge intensity	CI-mixing factor[d]	dipole strength D_0	covalency[e]
$[Fe^{III}Cl_4]^-$	2826.0[f]	2820.8[f]	5.2	1.51 ± 0.07[f]	1[f]	1.51 ± 0.07[f]	22 ± 1%
$[Fe^{II}Cl_4]^{2-}$	2825.0[f]	2823.1[f]	1.9	0.43 ± 0.04[f]	1/0.707[f]	0.60 ± 0.06[g]	9 ± 1%
$[Fe^{III}_2S_2Cl_4]^{2-}$	2825.6	2821.6	4.0	1.07 ± 0.09	1	1.07 ± 0.09	15 ± 1%
$[Fe^{2.5}_4S_4Cl_4]^{2-}$	2825.4	2821.8	3.6	1.03 ± 0.09	1	1.03 ± 0.09	15 ± 1%
$[Fe^{II}_2S_2Cl_4]^{4-}$ [h]	2824.8	2823.6	1.2	0.30	1/0.707	0.43	6%
$[Fe^{2.5}_2S_2Cl_4]^{3-}$ [i]	2825.2	2822.6	2.6	0.75	1	0.75	11%

[a] Inflection point reported is the highest-energy feature in the first derivative in the rising edge region. [b] Preedge energy given here is from fitting the data with several transitions. When more than one peak per transition is used to model the overall peak shape, the intensity-weighted average energy is given. [c] Calculated from the difference of the rising edge inflection point and the intensity-weighted preedge peak energy. Note that the given d-manifold shift is not an absolute number and can only be compared for the same ligands. [d] This factor accounts for the preedge intensity, which is shifted to higher energy by CI mixing with higher-lying states of the same symmetry as the electric-dipole allowed final states.[30] [e] Covalency is calculated using eq 3 and using D_{2d}-$[Cu^{II}Cl_4]^{2-}$ as reference (see text). The covalencies reported here are per metal−ligand bond. [f] From ref 30. [g] Note that there is an error in the computation of this value in Table 8 of ref 30. [h] Derivation of the values for this hypothetical ferrous dimer is given in the text. [i] Values of the hypothetical delocalized mixed-valence dimer are the mean values of the ferric and ferrous dimers (see text).

Table 3. Analysis of the S K-edges of Fe−S Clusters Containing Only Thiolate Sulfur and Relevant Reference Compounds

	rising edge inflection point[a]	preedge energy[b]	relative d-manifold energy shift[c]	preedge intensity	CI-mixing factor[d]	dipole strength D_0	covalency[e]
$[Fe^{III}(SPh)_4]^-$	2472.6	2470.2	2.4	1.03 ± 0.05	1	1.03 ± 0.05	38 ± 2%
$[Fe^{II}(SPh)_4]^{2-}$	2472.7	2471.4	1.3	0.39	1/0.700	0.55	21%
$[Fe^{III}_2Se_2(SPh)_4]^{2-}$	2472.7	2470.7	2.0	0.86 ± 0.05	1	0.86 ± 0.05	32 ± 2%
$[Fe^{2.5}_4Se_4(SPh)_4]^{2-}$	2472.5	2470.8	1.7	0.94 ± 0.04	1	0.94 ± 0.04	35 ± 2%
$[Fe^{II}_2Se_2(SPh)_4]^{4-}$ [f]	2472.8	2471.7	1.1	0.32	1/0.700	0.46	17%
$[Fe^{2.5}_2Se_2(SPh)_4]^{3-}$ [g]	2472.7	2471.1	1.6	0.66	1	0.66	25%

[a] Inflection point reported is the highest-energy feature in the first derivative in the rising edge region. [b] Preedge energy given here is obtained by fitting the data with several transitions. When more than one peak per transition is used to model the overall peak shape, the intensity-weighted average energy is given. [c] Calculated from the difference of the rising edge inflection point and the intensity-weighted preedge peak energy. Note that the given d-manifold shift is not an absolute number and can only be compared with that for the same ligand (here: thiophenolate). [d] This factor takes into account the preedge intensity which is shifted to higher energy by configuration interactions with higher-lying states of the same symmetry as those of the electric-dipole allowed final states. [e] Covalency is calculated using eq 3 and using the blue copper protein plastocyanin as reference (see text). The covalencies reported here are per metal−ligand bond. [f] Derivation of the values for this hypothetical ferrous dimer is given in the text. [g] Values of the hypothetical delocalized mixed-valence dimer are the mean values of the ferric and ferrous dimers (see text).

$(SPh)_4]^{2-}$, which has to be corrected for the change in oxidation state. The use of an experimental ferrous-to-ferric intensity ratio is hindered by lack of a well-determined preedge intensity in the ferrous monomer $[Fe^{II}(SPh)_4]^{2-}$. Thus, the calculated ferrous-to-ferric covalency ratio of 0.54 obtained from density functional calculations on $[Fe^{III}(SMe)_4]^-$ and $[Fe^{II}(SMe)_4]^{2-}$ is used.[71] Scaling the dipole strength of the ferric dimer with this ferrous-to-ferric ratio gives a dipole strength of 0.46 for the ferrous dimer $[Fe^{II}_2Se_2(SPh)_4]^{4-}$. Using the same ferrous-to-ferric intensity ratio, a dipole strength of 0.55 is estimated for the ferrous monomer $[Fe^{II}(SPh)_4]^{2-}$. The dipole strengths are converted into preedge intensities of 0.32 for the ferrous dimer and 0.39 for the ferrous monomer using a CI mixing correction factor of 0.700.[72] Estimated preedge peaks for the ferrous dimer $[Fe^{II}_2Se_2(SPh)_4]^{4-}$ at 2471.7 eV with an intensity of 0.32 and the ferrous monomer $[Fe^{II}(SPh)_4]^{2-}$ at 2471.5 eV with an intensity of 0.39 are included in Figure 4b, spectra 4 and 3, respectively.

Having established the properties of the hypothetical diferrous dimer, these values were then used in combination with the experimental energy and intensity values for the diferric compounds to estimate the properties of the hypothetical delocalized mixed valence dimer. Averaging the diferrous and diferric chloride (thiolate) values gives a rising edge inflection point of 2825.2 eV (2472.7 eV) and a relative d-manifold binding energy of 2.6 eV (1.6 eV). The difference in these values lead to the preedge energy of 2822.6 eV (2471.1 eV). Analogously, the dipole strength for the mixed valence dimer was determined as 0.75 (1.6).[75]

The dipole strengths of the mixed valence tetramer and dimer can be converted into covalencies by using eq 2.[75] This yields a covalency per $Fe^{2.5}$−Cl ($Fe^{2.5}$−SR) bond of 15% (35%) in the tetramer versus 11% (25%) in the hypothetical dimer. Thus, the $Fe^{2.5}$−Cl ($Fe^{2.5}$−SR) bond is 37% (40%) more covalent in the tetramer than in the dimer. The results of this analysis are

(71) The density functional calculations of $[Fe^{III}(SMe)_4]^-$ and $[Fe^{II}(SMe)_4]^{2-}$ give covalencies of 32.2 and 17.4%, respectively, compared to the experimental covalency of $[Fe^{III}(SPh)_4]^-$ of 38%. Considering the chloride monomers, the calculated covalency of $[Fe^{III}Cl_4]^-$ is 31.9% and of $[Fe^{II}Cl_4]^{2-}$ is 12.4% while the measured values are 22 and 9%, respectively. This shows that these density functional calculations overestimate the covalency of the Fe−Cl bond while slightly underestimate the covalency of the Fe−SR bond. The same trend was observed for Mo−Cl and Mo−SR covalencies in a previous study.[35] However, the calculated ferrous-to-ferric covalency ratio of 0.39 for the chlorides is identical to the one found experimentally (0.40). This supports the use of density functional calculations to estimate the ferrous-to-ferric covalency ratio.

(72) In analogy to the determination of the rescaling factor for preedge intensity shifted to higher energy by CI mixing for $[Fe^{II}Cl_4]^{2-}$,[30] this factor was determined for $[Fe^{II}(SPh)_4]^{2-}$. Using the Dq of $[Fe^{II}(S\text{-}2\text{-}Ph\text{-}Ph)_4]^{2-}$ [73] scaled down by 60% for the excited state[74] (210 cm^{-1}), the free ion B of Fe^{I} (722 cm^{-1}), and an e:t_2 covalency ratio of 0.625 (obtained from density functional calculations on $[Fe^{III}(SMe)_4]^-$) gives a correction factor for the intensity shifted to higher energy of 0.700.

(73) Gebhard, M. S.; Koch, S. A.; Millar, M.; Devlin, F. J.; Stephens, P. J.; Solomon, E. I. *J. Am. Chem. Soc.* **1991**, *113*, 1640−1649.

(74) Karpishin, T. B.; Gebhard, M. S.; Solomon, E. I.; Raymond, K. N. *J. Am. Chem. Soc.* **1991**, *113*, 2977−2984.

(75) To convert preedge intensity into covalency the possibility of CI mixing with higher lying states in the mixed-valence states has to be considered. Since there is no CI mixing with higher lying states in the diferric $[Fe^{III}_2S_2Cl_4]^{2-}$, the comparison of the preedge features of the mixed-valence tetramer $[Fe^{2.5}_4S_4Cl_4]^{2-}$ and the diferric dimer $[Fe^{III}_2S_2Cl_4]^{2-}$ gives an experimental measure of whether preedge intensity is shifted to the higher energy region in the mixed-valence tetramer. Overlaying the preedge peaks of these two compounds shows the same overall shape of these preedge features. Also, there is no additional higher-energy feature observable due to a higher lying state, which gains intensity through CI mixing with one of the parent excited states. Thus, no such effect is observed in the tetramers as expected for the delocalized mixed-valence dimer.

Table 4. Analysis of the S K-edges of Sulfide-Containing Fe−S Clusters

	rising edge inflection point[a]	preedge energy[b]	relative d-manifold energy shift[c]	preedge intensity	CI-mixing factor[d]	no. of metals bound to sulfide	dipole strength D_0	covalency[e]
$[Fe^{III}_2S_2Cl_4]^{2-}$	2474.0	2469.5	4.5	2.96 ± 0.10	1	2	1.48 ± 0.05	68 ± 2%
$[Fe^{2.5}_4S_4Cl_4]^{2-}$	2474.2	2470.1	4.1	2.57 ± 0.18	1	3	0.86 ± 0.06	39 ± 3%
$[Fe^{II}_2S_2Cl_4]^{4-}$ [f]		2470.7		1.06	1/0.700	2	0.76	35%
$[Fe^{2.5}_2S_2Cl_4]^{3-}$ [g]		2470.1		2.24	1	2	1.12	51%

[a] Inflection point reported is the highest-energy feature in the first derivative in the rising edge region. [b] Preedge energy given here is from fitting the data with several transitions. When more than one peak per transition is used to model the overall peak shape, the intensity-weighted average energy is given. [c] Calculated from the difference of the rising edge inflection point and the intensity-weighted preedge peak energy. Note that the given d-manifold shift is not an absolute number and can only be compared with that for the same ligands. [d] This factor accounts for the preedge intensity which is shifted to higher energy by configuration interactions with higher-lying states of the same symmetry as that of the electric-dipole allowed final states. [e] Covalency is calculated by using eq 3 and $CsFe^{III}S_2$ as reference (see text). The covalencies reported here are per metal−ligand bond. [f] Derivation of the values for this hypothetical ferrous dimer is given in the text. [g] Values of the hypothetical delocalized mixed-valence dimer are the mean values of the ferric and ferrous dimers (see text).

summarized in Tables 2 and 3. To illustrate these results, the estimated transition energies and intensities of the hypothetical dimers are included in Figure 4a and b using a Voigt line-shape.

B. Bridging Ligand: Sulfides. In this section the S−K preedge properties of the hypothetical delocalized mixed valence dimer $[Fe^{2.5}_2S_2Cl_4]^{3-}$ are estimated. As for the chloride and thiolate preedges, the properties of the mixed valence dimer were calculated as the average of the diferric $[Fe^{III}_2S_2Cl_4]^{2-}$ and diferrous $[Fe^{II}_2S_2Cl_4]^{4-}$ values. For the ferric dimer, the preedge intensity and the binding energies are taken from the measured spectrum, whereas the diferrous dimer has to be estimated. In contrast to the treatment of the thiolates and the chlorides, measured data are available for the Fe^{II}−sulfide unit in a dimer from S K-edge spectra of reduced spinach Ferrodoxin I (FdI).[65] Here, the Fe^{II}−sulfide peak does not overlap with the rising edge due to the decreased effective nuclear charge of the sulfide ligand as compared to the thiolate ligand. The flat preedge feature allows for deconvolution of the several transitions.[65] The preedge energy and intensity of this localized mixed valence dimer are corrected for the presence of the adjacent ferric site to derive the properties of a diferrous site as described below.

The estimation of the preedge energy of $[Fe^{II}_2S_2Cl_4]^{4-}$ is based on the Fe^{II}−sulfide preedge peak of the reduced $Fe^{II}Fe^{III}$ form of FdI at 2470.8 eV. This energy has to be corrected for the adjacent ferric site. This energy shift is estimated from the experimental energy shift of the Fe^{III}−sulfide preedge of FdI when the adjacent iron site is reduced from Fe^{III} to Fe^{II}, that is, going from the oxidized $Fe^{III}Fe^{III}$ to the reduced $Fe^{III}Fe^{II}$ form. This energy shift is scaled down by the ferrous-to-ferric energy shift ratio (0.57[68]) to obtain the ferrous energy shift when the adjacent iron center gets reduced. The Fe^{III}−sulfide preedge at 2469.7 eV in the diferric form shifts by only 0.2 eV to 2469.5 eV in the localized mixed valence form, mainly due to the decrease in effective nuclear charge of the sulfide. This procedure gives a preedge energy for the hypothetical ferrous dimer at 2470.7 eV.

The intensity of the preedge peak of the ferrous dimer is based on the experimental Fe^{II}−S preedge intensity of FdI. This intensity has to be renormalized[63] and corrected for intensity shifted to higher energy by CI mixing. The redistribution factor of 0.700 derived for ferrous thiolate is used. This approximation should be very good as the CI mixing correction factor does not change significantly on going from chloride (0.707) to thiolate ligation (0.700). This procedure gives a preedge intensity of 0.72 per Fe^{II}−sulfide bond. The intensity is expected to increase when the adjacent ferric ion is reduced. To account for this effect, the covalency change of the Fe^{II}−sulfide bond on going from $[Fe^{III}Fe^{II}S_2(SMe)_4]^{3-}$ to $[Fe^{II}_2S_2(SMe)_4]^{4-}$ is evaluated by density functional calculations. The effect is small and leads to a correction factor of 1.06. This yields a preedge intensity for the hypothetical diferrous unit of 0.76. An estimated preedge peak for $[Fe^{II}_2S_2Cl_4]^{4-}$ at 2470.7 eV with an intensity of 0.76 is added to Figure 4c as peak 2. This intensity value is a lower limit for the reduced dimer model because H-bonding in reduced FdI decreases the covalency of the bridging sulfide.[65]

The preedge feature of the hypothetical delocalized mixed valence dimer $[Fe^{2.5}_2S_2Cl_4]^{3-}$ is obtained by averaging the preedge energies and intensities of the measured ferric and the estimated ferrous dimer. This yields a preedge peak at 2470.1 eV with an intensity of 1.12 (again as a lower limit), which is given in Figure 4c.

The estimated intensity of the hypothetical delocalized mixed-valence dimer $[Fe^{2.5}_2S_2Cl_4]^{3-}$ and the measured intensity of the mixed-valence tetramer $[Fe^{2.5}_4S_4Cl_4]^{2-}$ lead to Fe^{II}−sulfide covalencies per bond of 51 and 39%, respectively.[75] This analysis is summarized in Table 4 and included in Figure 4c.

II. Covalency Dependence of Superexchange. In the following, an approximate relationship between the phenomenological superexchange coupling constant J and the covalency of the metal ions with the bridging ligand is obtained. The measured covalency difference can then be used to estimate the difference in the exchange coupling constants, which is needed to evaluate the different contributions to the delocalization behavior in the mixed-valence dimer and the tetramer. A simple perturbation approach is used, which is then tested using the VBCI model for superexchange.[76−79]

The simple model consists of a linear system with two metal sites, M_A and M_B, and one bridging ligand. The metals have one d-orbital each, and the ligand, one p-orbital ($|L\rangle$) (Figure 5). Two symmetry-adapted wave functions of the metal d-orbitals are constructed, $|g\rangle$ and $|u\rangle$. The *gerade* combination cannot interact with the ligand orbital and thus forms a nonbonding molecular orbital. The *ungerade* combination interacts with the ligand orbital creating a bonding molecular orbital, $|L\rangle^b$, with mainly ligand character and an antibonding molecular orbital, $|u\rangle^*$, with mainly d-orbital character. From perturbation theory, $|u\rangle^*$ can be written as

$$|u\rangle^* = |u\rangle - \frac{H_{ML}}{\Delta}|L\rangle \qquad (4)$$

The covalency of $|u\rangle^*$ is thus $(H_{ML}/\Delta)^2$. The energy difference

(76) Tuczek, F.; Solomon, E. I. *Inorg. Chem.* **1993**, *32*, 2850−2862.
(77) Tuczek, F.; Solomon, E. I. *J. Am. Chem. Soc.* **1994**, *116*, 6916−6924.
(78) Solomon, E. I.; Tuczek, F.; Root, D. E.; Brown, C. A. *Chem. Rev.* **1994**, *94*, 827−856.
(79) Brown, C. A.; Remar, G. J.; Musselman, R. L.; Solomon, E. I. *Inorg. Chem.* **1995**, *34*, 688−717.

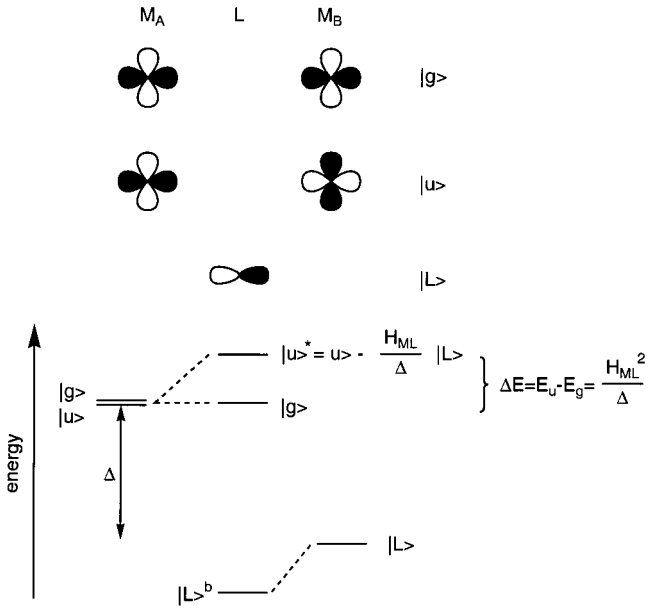

Figure 5. Model for the dependence of the superexchange coupling constant on covalency. The orbital basis consists of symmetry-adapted combinations of one d-orbital for each of the interacting metal sites and one p-orbital for the bridging ligand. The energy change and wave functions are given by perturbation theory.

between the mainly d-orbitals is the energy of destabilization of |u⟩*, which in second order is given by

$$\Delta E = E_u - E_g = \frac{H_{ML}^2}{\Delta} \tag{5}$$

From Hay, Thibeault, and Hoffmann,[80] the superexchange coupling constant is proportional to the square of this energy difference (eq 6).

$$J = \text{const}\,(E_u - E_g)^2 \tag{6}$$

Combining these equations gives

$$J = \text{const}\,\frac{H_{ML}^4}{\Delta^2} = \text{const} * \text{covalency}^2 * \Delta^2 \tag{7}$$

The magnitude of superexchange is thus proportional to the square of the covalency of the mainly metal d-derived molecular orbital. The covalency is also modulated by the square of the energy difference of the metal and ligand orbitals before interaction. It should be noted that this simple model is valid as long as there is no significant change in the bridging angle.

In the VBCI model for superexchange, the stabilization/destabilization of the different spin states is achieved by configurational interaction of a simple valence bond, localized ground-state configuration with higher-lying charge transfer configurations. In the theory of superexchange of Anderson, only the metal-to-metal CT, MMCT, states are considered.[81] This model provides a physical picture for antiferromagnetic coupling. To incorporate the pathway for superexchange through the bridging ligands, ligand-to-metal CT states, LMCT, were incorporated into the VBCI approach.[76−79] The LMCT states are energetically closer to the ground state as compared to the MMCT. Additionally, double ligand CT states, DCT, are included. The DCT and MMCT states couple through the LMCT with the ground state and are thus mixed into the ground state despite their high energy.

Scheme 4

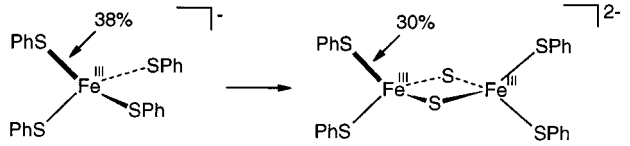

Scheme 5

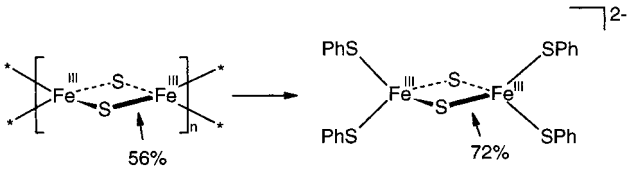

Covalency is introduced in the VBCI model by the amount of CI mixing of the LMCT into the VB ground state. To test the general applicability of eq 7, a VBCI calculation of the two coefficients in Figure 5 were performed. The value of J was calculated from the difference of the triplet and singlet VB ground states. The covalency was obtained from the square of the contribution of the LMCT configurations in the eigenvector of the ground state after full matrix diagonalization. The calculated coupling constant is plotted against the covalency in Figure S3a (Supporting Information). The resulting graph demonstrates the quadratic dependence of J on the covalency as expected from eq 7. The Δ^2 dependence of J was tested by varying the energy of the LMCT state and plotting J/covalency^2 against Δ. The resulting graph (Figure S3b) shows the quadratic dependence as predicted by eq 7.

Discussion

I. The Concept of Spectator Ligands. S K-edge spectra show that terminal ligands in Fe−S clusters can be used as spectator ligands for the electron density at the metal center when other ligands of the metal centers are changed. Scheme 4 illustrates this concept for terminal thiolate ligands where the numbers refer to the Fe^{III}−thiolate covalency per bond obtained by S K-edge XAS. The substitution of two terminal thiolates in $[Fe^{III}(SPh)_4]^-$ with two μ_2-bridging sulfides leads to the $[Fe^{III}_2S_2(SPh)_4]^{2-}$ dimer. Sulfides are stronger charge donors than thiolates, which is consistent with previous S K-edge studies[34] and chemical intuition. The stronger charge donation of the two sulfides in the dimer as compared to the two thiolates in the monomer increases the charge density at the Fe^{III} ion. Thus, from charge neutrality the remaining two thiolates donate less charge in the dimer (30% relative to 38% in the monomer). They serve as spectator ligands for the electron density at the metal center. Another example, where bridging sulfides are used as spectator ligands, is shown in Scheme 5. In this case substitution of two strong charge-donating μ_2-bridging sulfide ligands with two weaker charge-donating terminal thiolate ligands leads to a decrease in electron density of the Fe^{III} ion. Thus, the two remaining μ_2-bridging sulfides donate more charge, which is quantified by an increase of their Fe^{III}−sulfide covalency from 56% to 72%.

II. Covalency Differences of μ_2- and μ_3-bridging Sulfides. The properties of the Cl K-edge spectra of the terminal chloride ligands in the dimer $[Fe^{2.5}_2S_2Cl_4]^{3-}$ (estimated) and tetramer $[Fe^{2.5}_4S_4Cl_4]^{2-}$ (measured), the S K-edge spectra of the terminal

(80) Hay, P. J.; Thibeault, J. C.; Hoffmann, R. *J. Am. Chem. Soc.* **1975**, *97*, 4884−4899.
(81) Anderson, P. W. *Phys. Rev.* **1959**, *115*, 2−13.

thiolate ligands in $[Fe^{2.5}{}_2Se_2(SPh)_4]^{3-}$ (estimated) and $[Fe^{2.5}{}_4Se_4(SPh)_4]^{2-}$ (measured), and the S K-edge spectra of the bridging sulfide ligands in $[Fe^{2.5}{}_2S_2Cl_4]^{3-}$ (estimated) and $[Fe^{2.5}{}_4S_4Cl_4]^{2-}$ (measured) have all been used to probe the differences in the electronic structure on going from the mixed valence dimer to tetramer. The only change in each of these comparisons is the change in the bridging mode of the sulfide from μ_2 (in the hypothetical mixed-valence dimer) to μ_3 (in the experimental spectrum) (Scheme 2).

The illustrated differences in the Cl preedge properties of $[Fe^{2.5}{}_2S_2Cl_4]^{3-}$ (estimated) and $[Fe^{2.5}{}_4S_4Cl_4]^{2-}$ (measured) in Figure 4a are thus due to the effect of changing the bridging mode of the sulfide. On going from $[Fe^{2.5}{}_2S_2Cl_4]^{3-}$ to $[Fe^{2.5}{}_4S_4Cl_4]^{2-}$ the covalency of the terminal $Fe^{2.5}-Cl$ bond increases as indicated in the higher Cl preedge intensity of the tetramer in Figure 4a. This effect, which is quantified as 11% $Fe^{2.5}-$chloride covalency (estimated) in the dimer and 15% (measured) in the tetramer, is due to the change of the sulfide bridging mode. Using the terminal chlorides as spectator ligands, the electron density at the $Fe^{2.5}$ ion has decreased in the tetramer leading to an increased effective nuclear charge on the metal ion, which is compensated by the increased charge donation of the terminal chloride ligands. This effect is also reflected in the preedge energies. The preedge transition in the tetramer is at lower energy which is mainly due to the ~1 eV deeper d-manifold binding energy, that is, higher effective nuclear charge, in the tetramer. Thus, the μ_3-bridging sulfide in the tetramer is a weaker charge donor than the μ_2-bridging sulfide in the dimer.

The same effect is observed using the terminal thiolates as spectator ligands. The preedge peak of $[Fe^{2.5}{}_4Se_4(SPh)_4]^{2-}$ (measured) is more intense as compared to $[Fe^{2.5}{}_2Se_2(SPh)_4]^{3-}$ (estimated) (Figure 4b). The covalency of the terminal thiolate increases from 25% in the dimer to 35% in the tetramer. Again, this increase is the result of changing the bridging mode of the sulfide and shows that the μ_3-bridging sulfide in the tetramer is a weaker charge donor than the μ_2-bridging sulfide in the dimer. This effect is also present, but to a lesser extent, in the preedge energies of the thiolates. Generally, energy shifts are less pronounced in the S K-edges of thiolates as compared to the Cl K-edges of chlorides (Figure 4a and b).

The effect of changing the bridging mode of the sulfide can be seen directly (rather than indirectly via the spectator terminal ligands) in the sulfide preedge properties of the tetramer $[Fe^{2.5}{}_4S_4Cl_4]^{2-}$ (measured) and the hypothetical dimer $[Fe^{2.5}{}_2S_2Cl_4]^{3-}$ (estimated) (Figure 4c). On going from the dimer to the tetramer, the intensity of the preedge decreases (note that all the preedge peaks in Figure 4c are renormalized and display the intensity per bond). This is opposite to the trend observed for the terminal chloride and the thiolate ligands. The reduced covalency of the bridging sulfide is quantified by 39% in the tetramer as compared to 51% in the dimer (note that the covalency for the dimer is a lower limit, see Analysis section). Thus, binding a third iron center to the μ_2-bridging sulfide in the dimer leads to a reduction in the charge donation per $Fe^{2.5}-S$ bond. Chemically this is reasonable as a bridging sulfide, which additionally donates electron density to a third metal center, should, from charge neutrality, decrease its charge donation to the other two metal ions. It is important to note that the μ_3-bridging sulfide in the tetramer has, of course, a higher total covalency than the μ_2-bridging sulfide in the dimer (3 times the per bond covalency in the tetramer = 118% and 2 times the per bond covalency in the dimer = 103% total covalency). This is reflected in the sulfide preedge energies in Figure 4c. While in contrast with the chloride and thiolate preedge peaks in Figure 4a and b, the preedge of the tetramer is at the same energy as in the dimer, indicating that the shift in the d-manifold binding energy observed in the chloride and thiolate preedges is offset by a shift in the sulfide 1s core to deeper binding energy.

III. Effects on Superexchange. In this section the quantitative effect of the reduction in covalency of the bridging sulfides in going from the dimeric Fe−S clusters to the tetrameric Fe−S clusters on the superexchange contribution is discussed. In a recent study, the origin of the delocalization of the excess electron in the dimeric class III mixed-valence model compound $[LFe^{2.5}(OH)_3Fe^{2.5}L]^{2+}$ as compared to the localization in dimeric Fe−S clusters was found to be mainly due to the reduced superexchange interaction in the model compound.[24,25] Protonation of the bridges in the model compound weakens the charge donation to the metal and hence the superexchange. The exchange coupling in $[Fe_2S_2]^+$ was determined to be $J = -360$ cm^{-1} (this is the pure superexchange contribution, corrected for double exchange and vibronic coupling) and $J > -70$ cm^{-1} was established as a lower limit for $[LFe^{2.5}(OH)_3Fe^{2.5}L]^{2+}$.

To estimate the change in the superexchange contribution on going from the dimeric Fe−S cluster $[Fe_2S_2]^+$ to the tetrameric Fe−S cluster $[Fe_4S_4]^{2+}$, the superexchange coupling constant for $[Fe_4S_4]^{2+}$ is estimated by using eq 7 with the covalency ratio of the tetramer (measured) to the dimer (estimated) and the coupling constant of the localized mixed-valence dimer $[Fe_2S_2]^+$ as reference. The hypothetical mixed-valence dimer $[Fe^{2.5}{}_2S_2Cl_4]^{3-}$ estimated in the Analysis section is in the *delocalized* state (class III), whereas the reference mixed-valence dimer $[Fe_2S_2]^+$ is in the *localized* state (class II). Thus, the properties calculated for the delocalized dimer have to be related to the localized dimer. Density functional calculations on the mixed-valence dimer model $[Fe_2S_2(SMe)_4]^{3-}$ performed in the broken symmetry state and the high spin state show different covalencies of the bridging sulfides. The covalencies in the broken symmetry state are higher (35.4% sulfide covalency per bond) as compared to the high spin state (30.5%). The same trend is obtained for dimeric Cu^{II} complexes using a hybrid density functional.[82] Therefore, the experimentally estimated covalency of 51% for the delocalized dimer is scaled by 35.4/30.5 to estimate 60% covalency for the localized dimer.[83]

The superexchange constant is estimated using eq 7 with $J([Fe_2S_2]^+) = -360$ cm^{-1} and covalencies of 39% and 60% for the dimer subsite in the tetramer and the localized dimer, respectively, which gives a coupling constant for the dimer subsite of the tetramer of $J = -156$ cm^{-1}. The estimated covalency for the localized dimer is a lower limit (see Analysis section), so that the estimated coupling constant for the delocalized dimer subsite in the tetramer is a lower limit, that is, $J > -156$ cm^{-1}. Specific bonding interactions within the tetramer should further reduce this estimate of J for the dimer subsite. Tetrameric Fe−S clusters in the $[Fe_4S_4]^{2+}$ oxidation state are compressed along one S_4 axis giving overall D_{2d} symmetry. The Fe−S bonds connecting the two delocalized mixed-valence dimer subsites are shorter than the Fe−S bonds in the delocalized dimers subsites.[84] The covalency of the shorter

(82) Metz, M., Solomon, E. I., unpublished results.

(83) The covalency calculated for the broken symmetry state ($M_s = {}^1/_2$) is only a lower limit for the covalency of the pure $S_t = {}^1/_2$ spin state, because the broken symmetry state is a projection on the $M_s = {}^1/_2$ levels of all pure spin states.

(84) Berg, J. M.; Holm, R. H. in *Iron-Sulfur Proteins*; Spiro, T. G., Ed.; Metal Ions in Biology Vol. 4; John Wiley & Sons: New York, 1982; pp 1−66.

Table 5. Experimental Parameters Describing the Ground-state Magnetic and Valence-Delocalization Properties of $[LFe^{2.5}(OH)_3Fe^{2.5}L]^{2+}$, $[Fe^{2.5}{}_2S_2]^+$, and $[Fe^{2.5}{}_4S_4]^{2+}$

	$[LFe^{2.5}(OH)_3Fe^{2.5}L]^{2+}$	$[Fe^{2.5}{}_2S_2]^+$	$[Fe^{2.5}{}_4S_4]^{2+}$
J/cm^{-1}	>-70	-360	>-156
B/cm^{-1}	1350	965	1760
$\lambda^2/k_-/cm^{-1}$	2590	3660	3190

bonds should be larger than that of the longer bonds. The experimentally determined covalency is a mean value of these covalencies. Thus, the experimentally determined covalency for the tetramer gives an upper limit for the covalency in the delocalized dimer subsite of the tetramer. In summary, a lower limit (i.e., largest antiferromagnetic exchange coupling) for the superexchange interaction in the delocalized dimer subsite of the tetramer is established with $J > -156$ cm^{-1} (Table 5).

IV. Quantitative Analysis Including Double Exchange and Vibronic Coupling. To quantify the different delocalization−localization behavior of the mixed-valence dimer and the dimer subsite of the tetramer, the potential energy surfaces of the ground and excites states are evaluated by using eq 1, including the contributions from superexchange, double exchange, and vibronic coupling. In the following, the double exchange and vibronic coupling contributions on going from the dimer to the tetramer are estimated. The value of the double exchange contribution parametrized by B obtained for $[Fe_2S_2]^+$ is $B = 965$ cm^{-1}.[24,25] Noodleman and co-workers analyzed the double exchange contribution in Fe−S clusters by using density functional theory with different exchange-correlation functionals.[58,59,85,86] They found that the double exchange contribution increases on going from the dimer to the tetramer. The physical origin of this increase may be related to the butterfly twist on going from the dimer to the dimer subsite in the tetramer. Their most recent values for B obtained from the ground-state energy differences of the bonding and antibonding linear combinations of the d-orbitals representing the direct σ-delocalization pathway are $\sim$850 cm^{-1} in $[Fe_2S_2]^+$ and $\sim$1550 cm^{-1} in $[Fe_4S_4]^{2+}$.[60,87] Using the ratio of these numbers as a scaling factor on the value for $[Fe_2S_2]^+$ estimated from experiment (965 cm^{-1})[24] gives an estimate for $[Fe_4S_4]^{2+}$ of $B = 1760$ cm^{-1}.

For the analysis of the vibronic coupling contributions, the resonance Raman spectra and normal coordinate analysis of Spiro and co-workers were used.[88] The Q_- modes for the two dimer subsites of the tetramer which describe the antisymmetric breathing of each dimer transform as the E irreducible representation in the D_{2d} point group of the compressed tetramer. These delocalized Q_- modes are not normal modes of the molecule. The local Q_- mode projects onto several E normal modes of the tetramer. An estimate of these projections yields an approximate frequency for the localized Q_- mode in the dimer subsite of the tetramer of 290 cm^{-1}.[89] The vibronic coupling term λ^2/k_- is then calculated using eq 8

$$\frac{\lambda^2}{k_-} = 4\pi^2 c^2 M\, \tilde{\nu}_- n(\Delta r)^2 \qquad (8)$$

(with $M = 32$ au, $n = 4$, $\Delta r = 0.1$ Å, and $\tilde{\nu}_- = 290$ cm^{-1}) to be 3193 cm^{-1}. It is slightly reduced relative to the value obtained for $[Fe_2S_2]^+$ (Table 5). This is due to the combined effect of weakening the metal−sulfide bonds and strengthening the metal−thiolate bond.

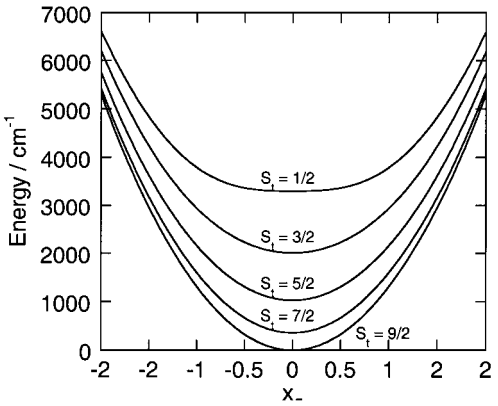

Figure 6. Energy dependence of the spin-states on Q_- of the delocalized dimer subsite in the mixed-valence tetranuclear Fe−S cluster in the dimensionless antisymmetric breathing mode x_- (calculated using eq 1 with the values given in Table 5).

Having established reasonable estimates for the superexchange, double exchange, and vibronic coupling contributions, the potential energy surfaces for the delocalized sub-dimer in the tetramer were calculated using eq 1. These are shown in Figure 6. The ground state is a delocalized $S_t = {}^9/_2$ spin state as determined experimentally. The values used for the superexchange contribution is a lower limit, and the value for the vibronic coupling is an upper limit (vide supra). Thus the contributions toward localization should be overestimated. Using these values for superexchange and vibronic coupling and fixing the double exchange parameter B to that of the localized mixed-valence dimer $[Fe_2S_2]^+$, a lower limit for the contribution toward delocalization, still yields a delocalized ground state for the mixed-valence dimer subsite in the tetramer but with an $S_t = {}^5/_2$ spin state.

Spin frustration in the tetrameric topology of course has a significant effect on the spin energetics of tetrameric Fe−S clusters and contributes to delocalization. However, it is important to note that a delocalized ground state can be obtained considering only the dimer subsite of the tetrameric Fe−S cluster. The main difference between the dimer sub-site of the tetramer and the dimer is the reduced covalency of the bridging sulfide ligands. This leads to a reduced superexchange which opposes delocalization. In this respect, protonation of the bridge in $[LFe^{2.5}(OH)_3Fe^{2.5}L]^{2+}$ gives a similar effect (Table 5) as the coordination of a third metal to the a μ_2-bridging ligand in the dimer to create a μ_3-bridging ligand in the tetramer. The pronounced reduction of the superexchange pathway associated

(85) Noodleman, L.; Case, D. A. *Adv. Inorg. Chem.* **1992**, *38*, 423−470.

(86) Li, J.; Noodleman, L.; Case, D. A. In *Inorganic Electronic Structure and Spectroscopy*; Solomon, E. I., Lever, A. B. P., Eds.; John Wiley & Sons: New York, 1999; Vol. I; pp 661−724.

(87) Knapp, M. J., Ph.D. Thesis, Department of Chemistry, University of California, San Diego, 1998, Chapter 5.

(88) Czernuszewicz, R. S.; Macor, K. A.; Johnson, M. K.; Gewirth, A.; Spiro, T. G. *J. Am. Chem. Soc.* **1987**, *109*, 7178−7187.

(89) The following normal modes (using the nomenclature of ref 88 where t stands for terminal and b for bridging and the irreducible representations in parentheses describe the symmetry in T_d) contribute to the Q_- mode: $E^t(T_2)$ at 360 cm^{-1}, $E^b(T_1)$ at 285 cm^{-1}, and $E^b(T_2)$ at 242 cm^{-1}. An estimate is made for these projections from the potential energy distributions, PED, given in ref 88. The two E^b modes are combined into one PED-weighted E^b mode, which is further combined with the E^t mode weighted by the 3/1 bridge-to-terminal ratio in the Q_- localized mode. The estimated value of 290 cm^{-1} is an upper limit because the different displacements of thiolate and sulfide in the monomeric breathing mode are not included ($\sim$0.7/1 for thiolate[84] relative to sulfide interpolated from the data given in refs 90 and 91).

(90) Segal, B. M.; Hoveyda, H. R.; Holm, R. H. *Inorg. Chem.* **1998**, *37*, 3440−3443.

(91) Morales, R.; Chron, M.-H.; Hudry-Clergeon, G.; Pétillot, Y.; Norager, S.; Medina, M.; Frey, M. *Biochemistry* **1999**, *38*, 15764−15773.

with reduced covalency is large enough to yield a delocalized ground state for the dimer sub-site of the tetramer.

Conclusions

The quantitative analysis of the ligand K-edge XAS spectra of dimeric and tetrameric Fe−S clusters gives the covalencies of the iron-ligand bonds. The change in electronic structure on going from the dimer to the tetramer due to the different bridging mode of the sulfide (μ_2 in the dimer vs μ_3 in the tetramer) is analyzed in detail. For this purpose, the ligand K-edge spectra of the chloride, thiolate, and sulfide ligands have been estimated for a hypothetical delocalized mixed-valence dimer. The difference between this dimer and the tetramers is then only the bridging mode of the sulfide (μ_2 vs μ_3). The covalencies of the terminal chloride and thiolate ligands increase on going from the dimer to the tetramer. Taking the terminal ligands as spectator ligands for the electron density at the formal $Fe^{2.5}$ ion indicates that the μ_3-bridging sulfides in the tetrameric Fe−S clusters are weaker charge donors than the μ_2-bridging sulfides in the dimeric Fe−S clusters. The decrease of sulfide covalency per bond is observed directly (in comparison to indirectly through spectator ligands) in the S K-edge spectra of the compounds with only sulfide ligation. The sulfide preedge peak of the tetramer is less intense than the sulfide preedge peak in the dimer. This trend is corroborated in the differences of the effective nuclear charge as observed from the energies of the preedge transitions. The reduction of covalency of the bridging ligand in the tetramers decreases the superexchange interaction between the iron centers. The superexchange is found to have a quadratic dependence on covalency allowing an estimate of the change in coupling constant for a μ_3- relative to a μ_2-bridge. Combining this with estimates of the change in the double exchange and vibronic coupling contributions on going from the dimer to the tetramer allows evaluation of the factors which lead to the localization in the mixed-valence dimer as compared to the delocalization in the mixed-valence dimer subsite of the tetramer. Our study shows that a major contribution to this change in the delocalization behavior is the reduction in covalency, and consequently in superexchange, on going from the μ_2-dimeric Fe−S clusters to the μ_3-tetrameric Fe−S clusters, which opposes the delocalization of the excess electron. This change in bridging-sulfide bonding should be included in understanding electron delocalization in the tetrameric Fe−S clusters along with models based on spin frustration.

Acknowledgment. This research was supported by NSF CHE-9980549 (E.I.S.) and by NIH RR-01209 (K.O.H.). Stanford Synchrotron Radiation Laboratory operations are funded by the Department of Energy, Office of Basic Energy Sciences. The SSRL Structural Molecular Biology Program is supported by the National Institutes of Health, National Center for Research Resources, Biomedical Technology Program, and by the Department of Energy, Office of Biological and Environmental Research. T.G. gratefully acknowledges the Deutsche Forschungsgemeinschaft for a postdoctoral fellowship. We also thank Professor. R. H. Holm, Harvard University for providing the compounds $[Et_4N]_2[Fe_4S_4(Smes)_4]$, $[n\text{-}Bu_4N]_2[Fe_4S_4(SPh)_4]$, $[Et_4N]_2[Fe(SPh)_4]$, and $[Et_4N][Fe(SPh)_4]$, Serena DeBeer for many helpful discussions and careful reading of the manuscript, Dr. Elodie Anxolabéhère-Mallart for many helpful discussions, and Dr. Louis Noodleman, UCSD, for providing results prior to publication.

Supporting Information Available: Figures S1, S2, and S3; input coordinates for DFT calculations (PDF). This material is available free of charge via the Internet at http://www.pubs.acs.org.

JA002183V